International Communications in Heat and Mass Transfer 124 (2021) 105242

Contents lists available at ScienceDirect

International Communications in Heat and Mass Transfer

journal homepage: www.elsevier.com/locate/ichmt

Recent progress on water vapor adsorption equilibrium by metal-organic frameworks for heat transformation applications

Sahrish Ashraf [a], Muhammad Sultan [a,b,*], Majid Bahrami [b], Claire McCague [b], Muhammad W. Shahzad [c], Mohammad Amani [b], Redmond R. Shamshiri [d], Hafiz Muhammad Ali [e]

[a] Department of Agricultural Engineering, Bahauddin Zakariya University, Bosan Road, Multan 60800, Pakistan
[b] Laboratory for Alternative Energy Conversion (LAEC), School of Mechatronic Systems Engineering, Simon Fraser University, Surrey, BC, Canada
[c] Mechanical and Construction Engineering Department, Northumbria University, Newcastle, Upon Tyne, NE1 8ST, UK
[d] Leibniz Institute for Agricultural Engineering and Bioeconomy, Max-Eyth-Allee 100, 14469 Potsdam, Bornim, Germany
[e] Mechanical Engineering Department, King Fahd University of Petroleum and Minerals, Dhahran 31261, Saudi Arabia

ARTICLE INFO

Keywords:
MOFs
Water vapors adsorption equilibrium
Cooling
Air-conditioning
Desalination

ABSTRACT

Adsorption-based heat transformation systems are studied from the twentieth century; however, their performance is low to replace conventional systems. Metal-organic frameworks (MOFs) are providing a new class of micro- and nano-porous organic adsorbents. These have adjustable geometry/topology with a large surface area and pore volume. A comparison of the coefficient of performance (COP) between the MOFs and conventional adsorbents-based cooling systems is made for the years 1975–2020. Conventional adsorbents achieve COP of 0.85, whereas it is improved to 2.00 in the case of MOFs. The main bottleneck in the lower COP level is the low adsorption equilibrium amount. This study is aimed to provide comprehensive detail of water-vapor adsorption equilibrium and physicochemical properties of hydrophilic MOFs. Zn based MOFs are not stable in the presence of water-vapors, whereas MIL series, Zr, Ni, and Cu based MOFs are relatively more stable. Among the studied MOFs, MIL-101(Cr) possesses the highest adsorption uptake of 1.45 kg/kg at 25 °C (saturation condition) and outperformed for heat transformation applications. Its uptake can be increased to 1.60 kg/kg by coating with graphite oxide. For water desalination, MIL-53(Al) exhibits specific daily water production of 25.5 m^3/ton.day (maximum) with a specific cooling power of 789.4 W/kg. Both MIL adsorbents are found promising which can be considered for various adsorption applications.

1. Introduction

Adsorption cooling and air-conditioning systems could be energy-efficient solutions for various applications compared to conventional technologies [1,2]. The performance of these systems is directly linked with adsorbent-adsorbate interactions [3,4] and the type of adsorption isotherms [5–7]. Thereby, the adsorbents' structure has a significant role in developing useful technologies [8,9]. Various adsorbent-adsorbate pair have been studied in the literature [10–12]. In this regard, the highest uptake was recorded by adsorption of difluoromethane

Abbreviations: A, adsorption potential [kJ/kg]; AlFs, aluminium fumarate; b, constant of Sips adsorption model [−]; BET, Brunauer-Emmett-Teller; COP, coefficient of performance [−]; COP_h, coefficient of performance of heating [−]; COP_{ref}, coefficient of performance of refrigeration [−]; D-A, Dubinin-Astakhov; DAC, desiccant air-conditioning; DE, dehumidification effectiveness; DSLF, dual site langmuir-freundlich; DUT, Duban University of Technology; DW, desiccant wheel; E, activation energy [kJ/kg]; GO, graphite oxide; H, constant of Freudlich adsorption model [kg/kg]; IUPAC, International Union of Pure and Applied Chemistry; MCHE, MOF coated heat exchanger; MIL, Material Institute Lavoisier; MOF, metal-organic framework; n, D-A model constant [−]; P, vapor pressure [kPa]; P/P_o, relative pressure [−]; PHCM, precise humidity control material; P_o, saturated vapor pressure [kPa]; P-T-W, pressure-temperature-concentration; R, general gas constant [kJ/kg.K]; RH, relative humidity [−] or [%]; SCHE, SGB coated heat exchanger; SCP, specific cooling power [W/kg]; SDWP, specific daily water production [ton/day/ton-ads]; SEM, scanning electron microscopy; SHG, second-harmonic generation; T, temperature [°C, K]; T_{con}, temperature of condenser [°C] or [K]; T_{eva}, temperature of evaporator [°C] or [K]; T_{in}, inlet temperature [°C] or [K]; UiO, University of Oslo; w, adsorption uptake [kg/kg]; w°, maximum adsorption uptake [kg//kg]; η_{deh}, dehumidification effectiveness [−].

* Corresponding author at: Department of Agricultural Engineering, Bahauddin Zakariya University, Bosan Road, Multan 60800, Pakistan.
E-mail addresses: muhammadsultan@bzu.edu.pk, muhammad_sultan@sfu.ca (M. Sultan).

https://doi.org/10.1016/j.icheatmasstransfer.2021.105242

Available online 31 March 2021

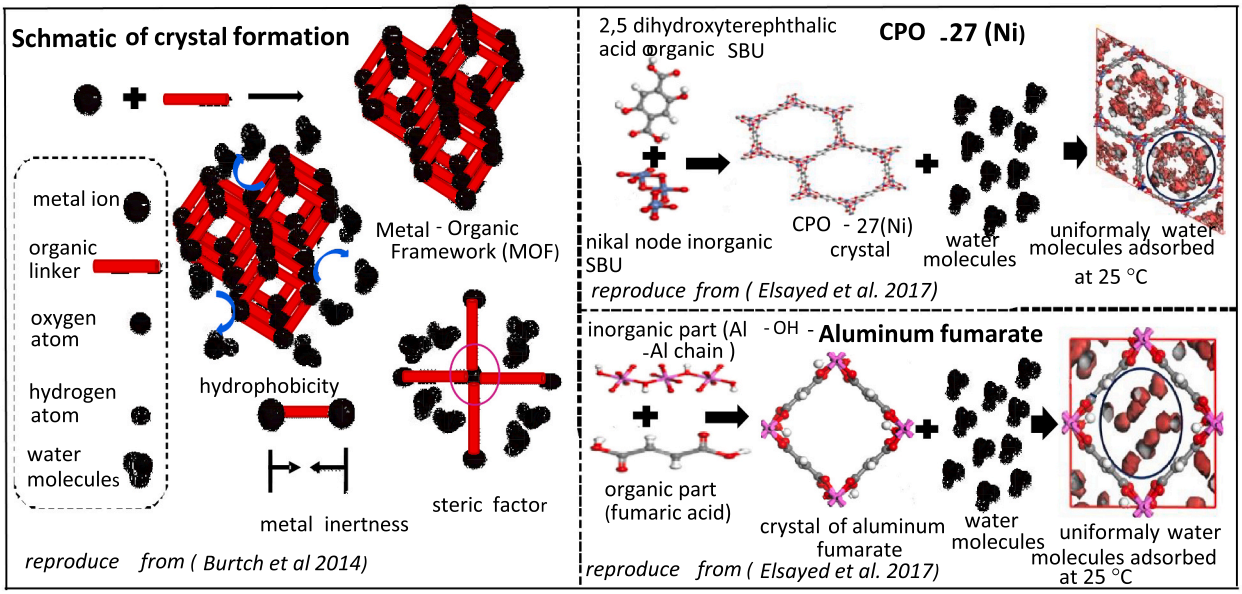

Fig. 1. Fundamental of MOFs crystal formation along with water-vapor interaction (left). The basic unit of crystal formation and change in crystal after water-vapor adsorption for CPO-27(Ni) (top right), and aluminium fumarate (bottom right), reproduced from [50,80].

(HFC-32) onto phenol resin-based adsorbent [13]. Water vapor adsorption has been studied for various adsorbents [14,15] e.g. silica-gel [16–18], activated carbon [19,20], polymers [21–24] and zeolite [25–28]. These hydrophilic adsorbents are investigated for many applications e.g. silica-gel for greenhouse air-conditioning [29], drying of agricultural products [30,31], thermal energy storage system [32], and adsorption cooling/air-conditioning [16,33]; activated carbons and silica gel for greenhouse air-conditioning [29], adsorption refrigerator [34,35], air-conditioning [36], and ice-making [37]; polymers for desiccant air-conditioning (DAC) [38]; and zeolites for heat storage [26] and air-conditioning [39,40]. The adsorbents' hydrophobicity is greatly concerned with surface area and volume of macro-, meso-, micro and nano-pores to welcome incoming molecules of water-vapors [41]. In this regard, metal-organic frameworks (MOFs) are a new class of micro- and nano-porous adsorbents with exclusive adsorption properties [14,42]. These are known as porous coordination polymers, metal-organic materials and organic coordination polymers [43–46].

The MOFs are hybrid adsorbents in which organic linkers connect with inorganic metal ions by coordination; metal ions provide more stability to crystals and enhance their hydrophilic character. Metal nodes in MOFs increase flexibility and side spaces [49], providing many ways to synthesize many adsorbents with the same organic linker. According to the Cambridge database [47], nearly 12,000 MOF structures have been synthesized until now using 102 organic linkers with different metal nodes. They have a more flexible structure design with the greater ability to control pore functionalization than other organic adsorbents like zeolite and polymers. Furthermore, the MOFs have an organic part in their solid structure formation, making them more versatile than zeolite [48]. A simple schematic of the MOFs formation is shown in Fig. 1. It can be observed that MOFs crystal formed cage-like 3-dimensional open-spaced structure due to the support of metal ions and possess huge accessible free space to attract water molecules. A simple schematic of crystal formation and adsorption of water-vapor for CPO-27(Ni) and aluminium fumarate (AlFs) is also shown in the figure. It can be observed that these adsorbents possess more fluctuations in structure and crystal design while interaction with water vapors. Many experimental studies showed that MOFs had higher water-vapor uptake than conventionally used adsorbent, e.g. silica-gel [49,50]. There is a functional relationship between the adsorbent structure and the amount of adsorption equilibrium investigated in the literature [51–53]. Moreover, the surface area, pores volume, and structural stability of the MOFs may significantly affect the water-vapor adsorption equilibrium [54–56]. Water-vapor adsorption uptake can be improved by coating the adsorbents with other metal(s) [57]. For example, adsorption uptake of MIL-101(Cr) has increased 1.07 times when coated with graphite oxide (GO) at 25 °C and 0.90 relative pressure, as its surface area increased from 2489 to 3522 m^2/kg [58–60].

Various studies has been conducted to synthesized and characterized the MOFs in term of water-vapor adsorption equilibrium e.g. MOF-5 [43,61,62], HKUST-1 [56,63], CPO-27(Ni, Cr, Cd, Mg) [49,52,53,64,65], MIL-(101, 100, 125) [54,66,67] and zirconium-based MOFs [68,69]. Therefore, this study aims to provide a brief comparison of the MOF adsorbents that can be helpful in selecting a suitable adsorbent according to thermophysical and thermodynamic properties. Several studies on MOFs/adsorbates interaction have been reported in the literature using close and open-cycle adsorption cycles [70] for cooling [71–74] and air-conditioning [53,60] applications. In the case of open-cycle applications, MOFs adsorption uptake is supposed to be limited to water-vapors [60], whereas, in the case of close-cycle applications, MOFs adsorption have been reported with various adsorbates, e.g. water-vapors [53,72], ethanol [75–77] and methanol [73,78]. However, in each case, adsorption equilibrium uptake and adsorption kinetics are key adsorption properties for developing a real system [79]. Adsorption uptake of ethanol onto MIL-101 has been reported as high as 1.10 kg/kg (at 25 °C) [77] and 0.74 kg/kg (at 25 °C)) [75] and methanol onto HKUST-1 and MIL-101 yielded 0.55 kg/kg (at relative pressure of 0.90) and 1.20 kg/kg (at relative pressure of 0.80), respectively [73]. Similarly, MOF yielded higher methanol adsorption uptake and performance at lower heat rejection and evaporator temperature than activated carbon. This higher adsorption uptake of ethanol significantly increases the coefficient of performance (COP) and specific cooling power (SCP) of the systems. In each case, MOFs possess higher cyclic stability e.g. MIL-101/ethanol stable after 60 adsorption/desorption cycles [75] and MIL-101(Cr)/methanol can be applicable up to 1000 adsorption/desorption cycles [73].

Hydrophilic MOFs have been reported many close-cycle applications including water desalination [50,52,81], adsorption heat pump and adsorption chillers [49,55,82], heat transformation and storage [67,69,83,84], solar energy storage [85], humidity control [86], adsorption cooling and air-conditioning [53,71,72,87], pollutant

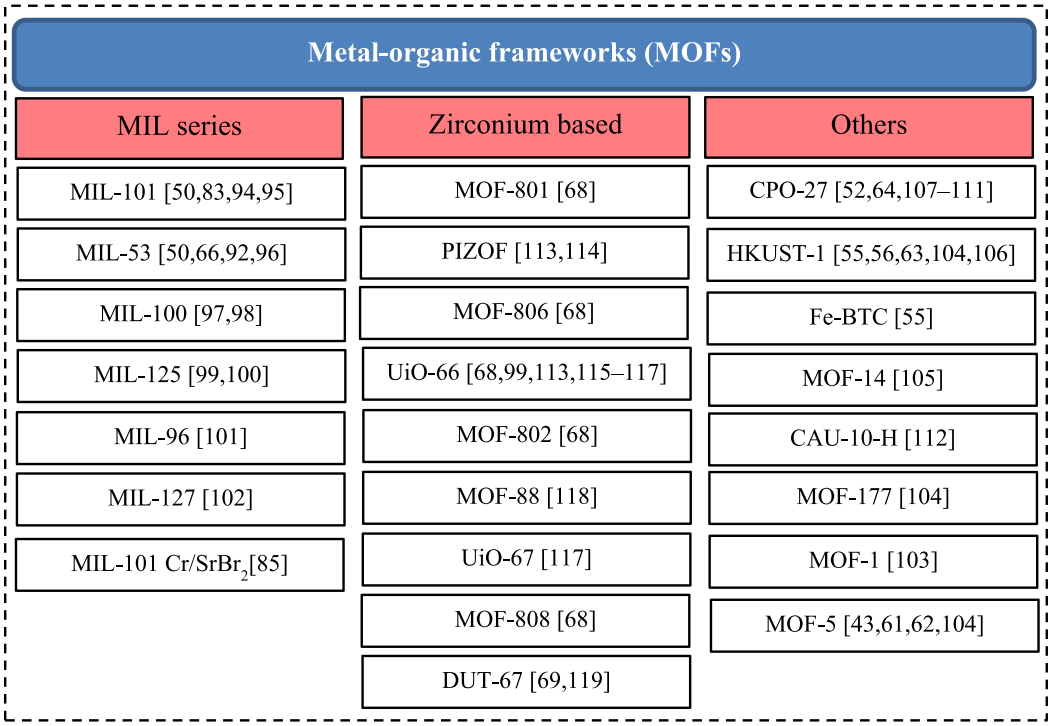

Fig. 2. Overview of the MOF adsorbents studied in the literature.

removal [88], and ice-making [81]. In an experimental study [53], CPO-27(Ni) has 1.23 times higher water-vapor adoption uptake than silica-gel when investigated for automobile air-conditioning, resulting in COP and SCP of the system as 0.26 and 105 W/kg, respectively. Similarly, hydrophilic MOFs have been investigated for many open-cycle application, e.g. water harvesting [89,90], moisture sensing [91], wastewater treatment [92,93] and air-conditioning [60]. In a simulation study [60], MIL-101(Cr) investigated for open-cycle air-conditioning purposes and results showed that MIL-101(Cr) outperformed silica-gel.

In this regard, many studies have been reported in the literature to investigate the performance of these materials, highlighting their potential use in many applications. This study aimed to review the water-vapor adsorption equilibrium of hydrophilic MOFs available in the literature and their potential to use for adsorption based cooling and air-conditioning applications.

2. Adsorption characteristics of MOF/water pairs

This study reviewed various kinds of MOF based hydrophilic adsorbents which were synthesized and characterized in the literature e.g. MIL-101 [50,83,94,95], MIL-53 [50,66,92,96], MIL-100 [97,98], MIL-125 [99,100], MIL-96 [101], MIL-127 [102], MIL-101 Cr/SrBr2 [85], MOF-1 [103], MOF-5 [43,61,62,104], MOF-14 [105], HKUST-1/MOF-199 [55,56,63,104,106], CPO-27 [52,64,107–111], CAU-10-H [112], MOF-177 [104], Fe-BTC [55], MOF-801 [68], PIZOF [113,114], MOF-806 [68], UiO-66 [68,99,113,115–117], MOF-802 [68], MOF-88 [118], UiO-67 [117], MOF-808 [68], DUT-67 [69,119]. The details of the adsorbents are provided in Fig. 2.

2.1. Physical characteristics and chemistry

The MOFs are formed by the coordination of organic linkers and metal ions. These metal ions act as a base, while organic linker act as a bridging unit. The strong coordination between metal ions and organic linkers is a key factor to make a stable crystal. The crystal stability makes these adsorbents more versatile and unique than other adsorbents. Crystal and structural properties of MOFs based adsorbents with good water vapors adsorption uptake are shown in Table 1. Many crystals have uniformly connected each other to form a huge molecule with empty spaces. However, the presence of empty spaces on each side makes these adsorbents more reactive and unstable. They can easily react to chemicals and moisture present in the air during their preparation process. Therefore, it is necessary to achieve control conditions in the laboratory during their preparation. Water molecules get attached to the crystals when these adsorbents are completely synthesized. Heat treatment is required to remove excessive water molecules from the crystals [120]. This heat treatment inactivates the adsorbents and makes them more thermally and chemically stable, e.g. HKUST-1 and MIL-101 have thermal stability of 240 °C and 275 °C, respectively [63,95].

Various studies highlighted hydrophilic character and higher hydrothermal stability of these adsorbents, e.g. nickel-based CPO-27 [50,53,107]. Some of the MOFs may be hydrophobic and possessed a higher attraction for other adsorbate molecules. For example. MOF-5 is not moisture stable, but it can be utilized for gas separation applications [61]. The hydrophilic and hydrophobic character can be determined by the type of metal ions and nature of interaction with the organic linker and metal ions. Fig. 3(a)-(d) [128] gives a brief insight into the geometries of clusters transition states upon ligand hydrolysis/displacement reaction in MOF-5, HKUST-1, MIL-101 and ZIF-8, respectively. Besides, a simple water stability map of different MOFs materials is shown in Fig. 3(e) [121]. Some of the adsorbents of this class are moisture sensitive and degraded when exposed to water-vapors. It is because of the type of metal node, e.g. Zn metal-based MOFs are moisture sensitive [104]. Similarly, MOF-5 is not stable in the presence of moisture and degraded at a relative humidity (RH) of more than 4% [61]. Additionally, some of the adsorbents are stable at lower relative pressure range and start to degrade at high relative pressure, e.g. HKUST-1 (also known as CuBTC/MOF-199 [65]) is more moisture stable at lower relative pressure [56]. It is due to the presence of copper (Cu) metal ions which are moisture stable. The bond length (Cu—Cu bond) starts to elongate when water-vapors contact with its crystal [59], and bond length elongation increases continuously when the number of water-vapor

Table 1
Details about the structure and physical properties of the studied MOFs.

MOF class	MOF name	SEM or SHG image	Crystal structure	Chemical formula	Physical properties		
					Surface Area (m^2/g)		Pores volume (cm^3/g)
					BET	Langmuir	
CPO-27/MOF-74	CPO-27 (Ni)	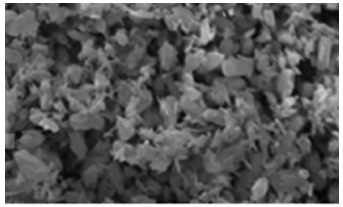 [52]	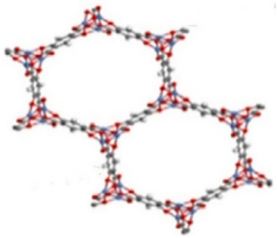 [52]	$Ni_2(dhtp)(H_2O).8H_2O$ [107]	1113 [110] 1337 [108]	N/A	0.39 [110] 0.54 [108]
MIL-101	MIL-101-Cr	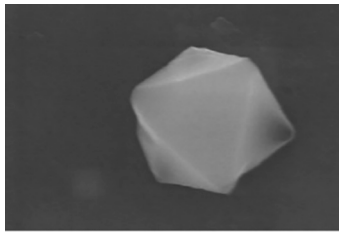 [94]	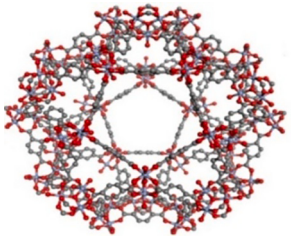 [50]	[Cr3(O)(BDC)3(F,OH)-(H_2O)2] [83]	4000 [83] 2789 [94]	4500–5500 [95]	1.51 [85]
Composite MIL-101(Cr) @GO	MIL-101(Cr) @GO-2	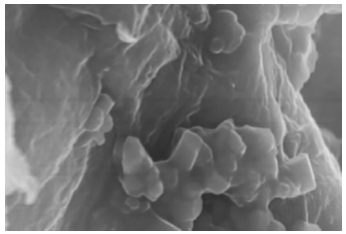 [94]	N/A	N/A	3472 [94]	5031 [94]	1.69 [94]
HKUST-1/ CuBTC/MOF-199	HKUST-1/ CuBTC/MOF-199	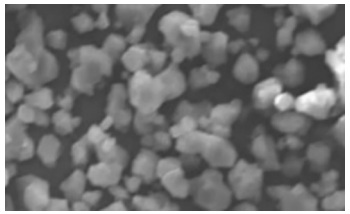 [55]	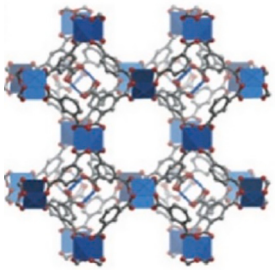 [104]	$C_{18}H_6CH_3O_{12}$ [55] $Cu_3(C_9H_3O_6)_2$ [104]	1500–2100 [55] 1568.5–2081.5 [106]	917.6 [63]	0.75 [106]
CAU-10	CAU-10-H			[Al(OH)(O_2C-C_6H_4-CO_2)]0.1.7H_2O:C 40.2%, H 3.1% [112]	S_{BET} = 635 [112]	N/A	0.23 [112]

(*continued on next page*)

Table 1 (*continued*)

MOF class	MOF name	SEM or SHG image	Crystal structure	Chemical formula	Physical properties		
					Surface Area (m^2/g)		Pores volume (cm^3/g)
					BET	Langmuir	
		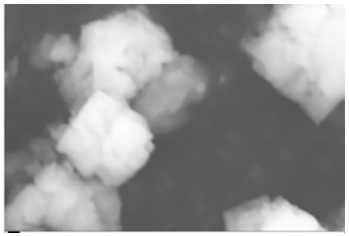 [112]	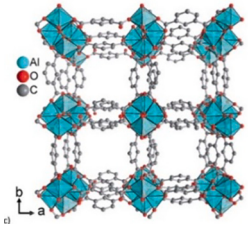 [124]				
Zirconium based MOFs	UiO-66	N/A	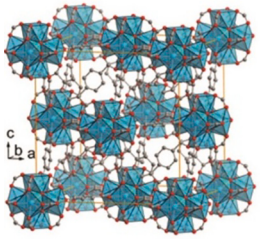 [99]	$Zr_6O_4(OH)_4(BDC)_6$[68]	1290 [68]	1187 [125] 1030 [99]	0.49 [68] 0.52 [99]
	UiO-66-NH_2	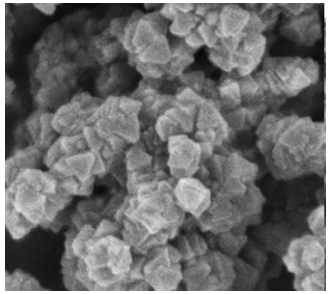 [93]	N/A	N/A	905 [93]	N/A	0.43 [93]
	MOF-801-P	N/A	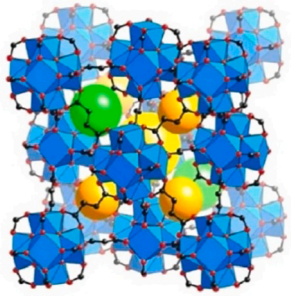 [68]	$Zr_6C_{24}H_{28}O_{38}$ $Zr_6O_4(OH)_4(fumarate)_6$ [68]	990 [68]	1070 [68]	0.45 [68]
	MOF-801-SC	N/A	N/A	$Zr_6C_{24}H_{28}O_{38}$ $Zr_6O_4(OH)_4(fumarate)_6$ [68]	690 [68]	770 [68]	0.27 [68]

(*continued on next page*)

Table 1 (*continued*)

MOF class	MOF name	SEM or SHG image	Crystal structure	Chemical formula	Physical properties		
					Surface Area (m^2/g)		Pores volume (cm^3/g)
					BET	Langmuir	
	MOF-805	N/A	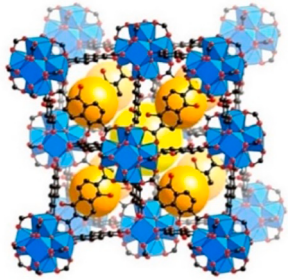 [68]	$Zr_6O_4(OH)_4[NDC\text{-}(OH)_2]_6$ [68]	1230 [68]	1370 [68]	0.48 [68]
	MOF-806	N/A	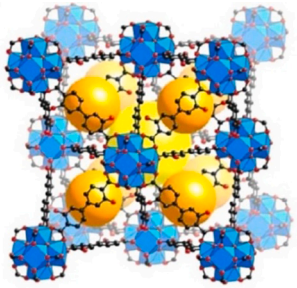 [68]	$Zr_6O_4(OH)_4[BPDC\text{-}(OH)_2]_6$ [68]	2220 [68]	2390 [68]	0.85 [68]
	MOF-812	N/A	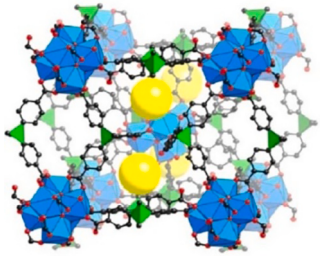 [68]	$Zr_6O_4(OH)_4(MTB)_3(H_2O)_2$ [68]	N/A	N/A	N/A
	MOF-802	N/A	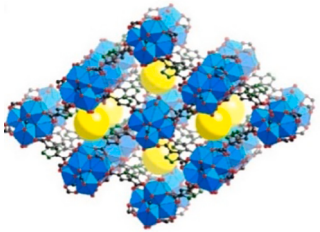 [68]	$Zr_6O_4(OH)_4(PZDC)_5(HCOO)_2(H_2O)_2$ [68]	<20 [68]	<20 [68]	<0.01 [68]
	MOF-841	N/A			1390 [68]	1540 [68]	0.53 [68]

(*continued on next page*)

Table 1 (*continued*)

MOF class	MOF name	SEM or SHG image	Crystal structure	Chemical formula	Physical properties		
					Surface Area (m^2/g)		Pores volume (cm^3/g)
					BET	Langmuir	
			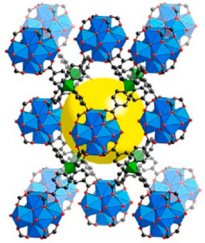 [68]	$Zr_6O_4(OH)_4(MTB)_2(HCOO)_4(H_2O)_4$ [68]			
	MOF-808	N/A	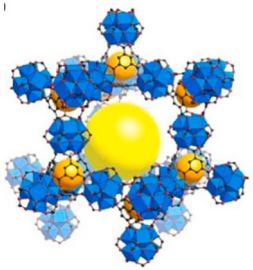 [68]	$Zr_6O_4(OH)_4(BTC)_2(HCOO)_6$ [68]	2060 [68]	2390 [68]	0.84 [68]
MIL-125	MIL-125 Material institute Lavoisier	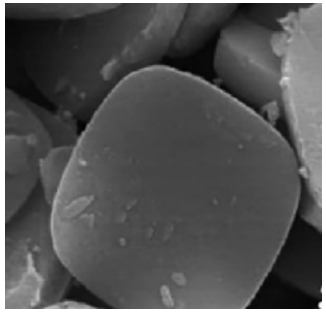 [100]	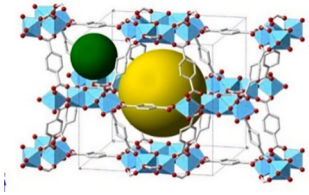 [100]	N/A	1510 [100]	N/A	0.68 [100]
	MIL-125-NH_2	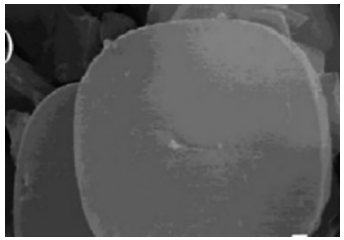 [100]	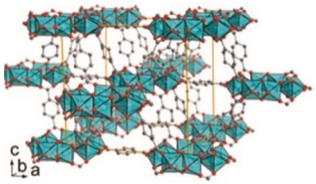 [99]	$Ti_8O_8(OH)_4H_2N$-$(BDC)_6$ [99]	1469 [100] 859 [99]	N/A	0.60 [100] 0.53 [99]
MIL-53				[Al(OH)(O2C CH CH CO2)] [92]		1000–1200 [96]	

(*continued on next page*)

Table 1 (*continued*)

MOF class	MOF name	SEM or SHG image	Crystal structure	Chemical formula	Physical properties		
					Surface Area (m^2/g)		Pores volume (cm^3/g)
					BET	Langmuir	
	Aluminium Fumarate MIL-53-Al	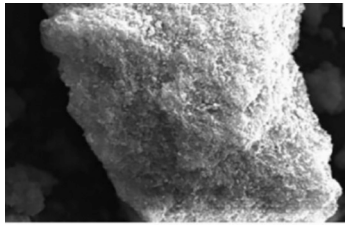 [92]	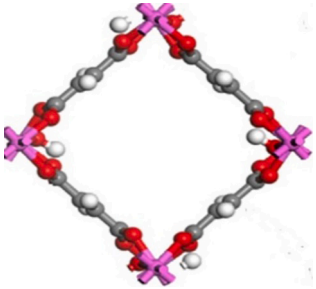 [50]		792.26 [66] 1021 [96]		0.926 [66] 0.48 [96]
	MIL-53-Ga	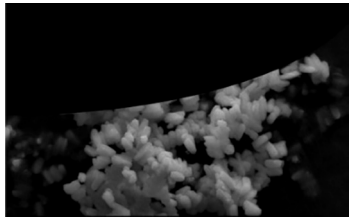 [126]	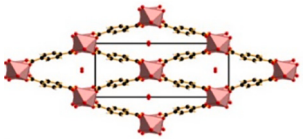 [127]	$Ga(OH)_{0.9}(F)_{0.1}(BDC)0.0.9H_2O$ [128]	N/A	N/A	N/A
CAU-13	CAU-13-Ga	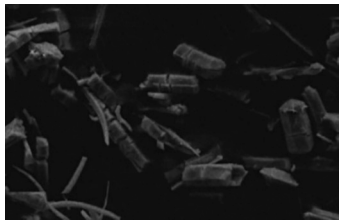 [126]	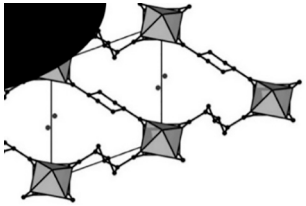 [126]	N/A	N/A	N/A	N/A
MIL-100	MIL-100-Fe	N/A	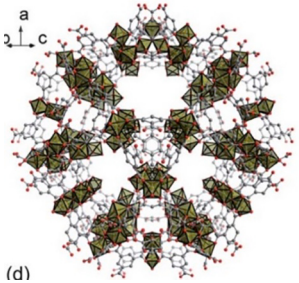 [97]	N/A	1917 [97]	N/A	1.00 [97]
	MIL-100-Cr	N/A		N/A	1130 [98]	N/A	0.77 [98]

(*continued on next page*)

Table 1 (*continued*)

MOF class	MOF name	SEM or SHG image	Crystal structure	Chemical formula	Physical properties		
					Surface Area (m^2/g)		Pores volume (cm^3/g)
					BET	Langmuir	
			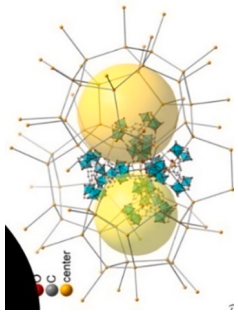 [98]				
	Fe-BTC	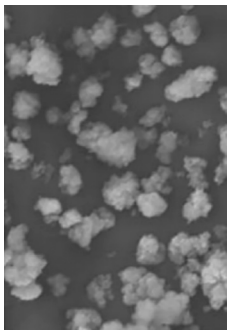 [55]	N/A	$C_9H_3FeO_6$ [55]	1300–1600 [55]	N/A	N/A

Key: N/A: not available; S_{BET}: specific BET surface area.

molecules increases. Therefore, HKUST-1 shows relatively higher water-vapor uptake at lower relative pressure and unstable at higher relative pressure. However, changing metal ions with the same organic linker can alter adsorptive and physical characteristics. For example, MOF-74 [111], also known as CPO-27 [64,65], developed by the coordination of 2nd group transition metal ions (Mg, Ni, Cd, Cu and Cr) with 2,5-dioxide-1,4-benzenedicarboxlyte organic linker [64,107–109]. Moisture stability in CPO-27 is determined by metal and oxygen (M-O) bond strength [122]. Bond length elongation is large in the case of Cr, Cd, Mg and Cu metals. While the M-O bond elongation is negligible in Ni metal ion and crystal retained its original position when it dehydrated. Hence, CPO-27(Ni) found to be more stable in the presence of water-vapors [107].

Crystal formation/deformation in the presence of water-vapors in the MIL series is observed, which is quite different from other studied MOFs adsorbents. Most of the MIL series's adsorbents attracted fewer water-vapors at lower relative pressure ranges (0.10 to 0.30) compared to higher relative pressure (0.50 to 0.90) [59,71,94]. For examples, MIL-101 and MIL-100 have started to absorb water-vapors at relative pressure ranging from 0.30 to 0.40. Similarly, aluminium (Al) and gallium (Ga) metal(s)-based MOFs were found to be water-vapor stable as compared to other metal ions-based adsorbents. For example, AlFs [92] showed a honeycomb-like flexible structure with more surface area due to long repeating (-Al-O-Al-O-Al-O-Al-) chains. Therefore, water-vapors can easily attach to the crystal without deformation. Thus, the crystal retained their original position when dehydrated or thermally treated. Similarly, zirconium (Zr)-based MOFs like UiO-66 is formed from the octahedral group of $Zr_6O_4(OH)_4$ with BDC linker has possessed higher moisture stability [123].

2.2. Water-vapor adsorption equilibrium

The MOFs usually exhibit continuous water-vapor adsorption uptake at all RH ranges due to the macro, *meso* and micro pores' availability in their crystals. Water vapors were firstly settled into macropores, followed by meso and micro pores. The MOFs usually exhibited various types of water-vapor adsorption isotherms.

MOFs of the MIL series are extensively studied in the literature, which exhibited adsorption isotherms of type-IV and type-V as per IUPAC classification. Water-vapor adsorption uptake of Al-based MIL-53 (known as AlFs) was investigated in the literature [50]. Al and Ga metal-based adsorbents were found to be more stable for water vapor adsorption due to Al and Ga metals' water stability. MIL-53(Al) showed uptake of 0.36 kg/kg at relative pressure of 0.90 with adsorption isotherm of type-IV [49,50,129]. Dubinin-Astakhov (D-A) based equations (Table 3) were used depending upon the adsorption potential range to model the adsorption equilibrium data. The adsorption uptake behavior of MIL-53(Ga) was quite different from MIL-53(Al) due to the presence of a large number of hydrated nano-pores in its crystals [130]. Moreover, iron (Fe) and chromium (Cr) based MIL-53 have not shown good water vapor adsorption uptake [55]. The Cr and Fe metal ions have shown more attraction for water-vapors than the organic linker and resulted in adsorbents degradation. Chromium-based MIL-101 possessed an uptake of 1.45 kg/kg at relative pressure of 0.90 [50]. It exhibited type-V adsorption isotherm, and D-A based equations (depending upon relative pressure range) were used to fit adsorption equilibrium data as presented in Table 3.

The adsorption properties can be improved by changing/adding functional groups/ coating material with other hydrophilic metal(s) [94,131]. For example, the adsorption uptake of MIL-101 was improved to 1.60 kg/kg at a relative pressure of 0.90 when coated with GO to form MIL-101(Cr)@GO [58,60,98]. Similarly, water-vapor adsorption uptake of MIL-100 was investigated with aluminium and iron metals ions [96,132]. MIL-100(Fe) shown maximum uptake of water vapors of 1000 cm^3/g (at 273 K) and exhibited type-V adsorption isotherm, which is relatively higher (i.e. 0.70 kg/kg) as compared to MIL-100(Al) (i.e. 0.48

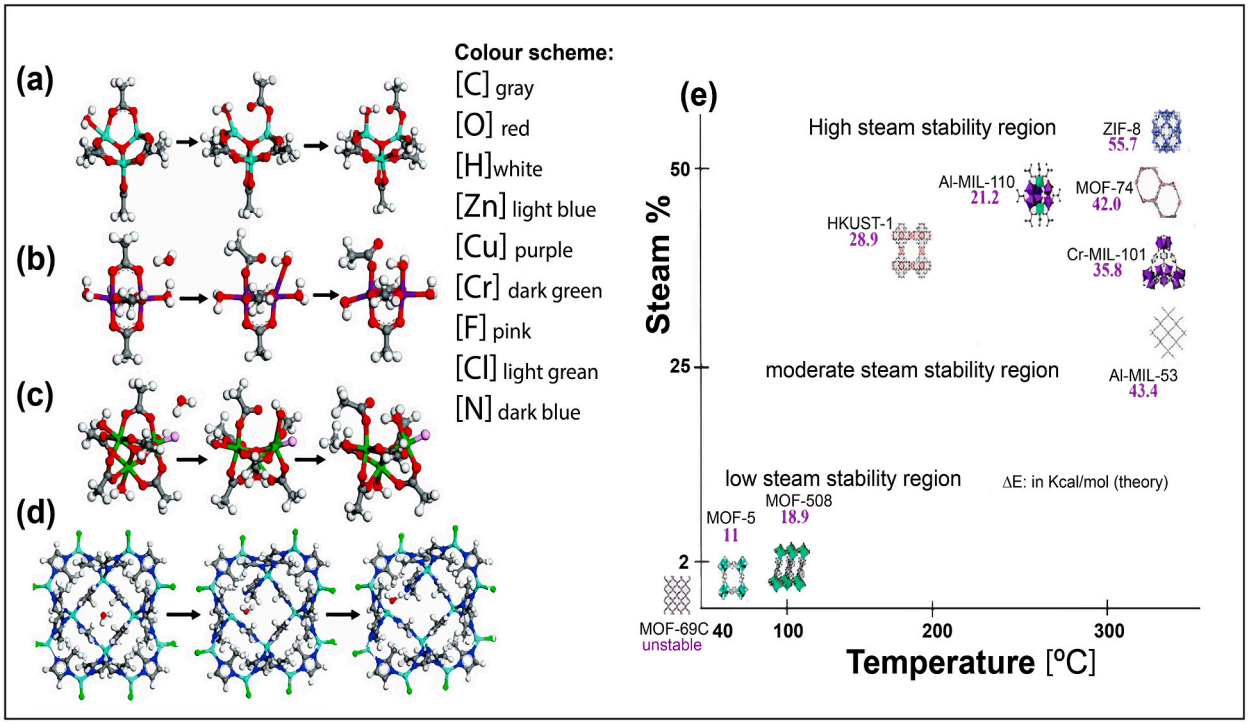

Fig. 3. A brief insight of the geometries of clusters transition states upon ligand hydrolysis/displacement reaction in (a) MOF-5, (b) HKUST-1, (c) MIL-101 and (d) ZIF-8; (e) a general stability sketch of MOFs in the presence of water molecules [121].

kg/kg) at 273 K and relative pressure of 0.90. MIL-100(Fe) had large hysteresis at the same temperature and relative pressures. It had high hydrothermal stability as it is stable after 40 adsorption/desorption cycles and 5 h per cycle at the temperature range from 40 to140 °C [97]. MIL-125 with functional group H_2N shown uptake of 0.60 kg/kg (at a relative pressure of 0.9 and 273 K) and owning to adsorption isotherm of type-IV [99]. A detailed comparison of water-vapor adsorption isotherms for MIL series-based MOFs is provided in Fig. 4 (a). MIL-101 with Cr templet has shown the highest water-vapor adsorption uptake than all other adsorbents of the MIL-series. A noticeable increase in the adsorption uptake can be observed when MIL-101(Cr) was coated with Graphite oxide (GO) that increased adsorption uptake ability and stability.

Similarly, Zr-based MOFs, e.g. MOF-801, MOF-805, MOF-806, MOF-802, MOF-841, MOF-812 and MOF-808, were also investigated, which shown reasonable water-vapor adsorption uptake [68,114]. Adsorption behavior of some Zr-based adsorbents was compared in a study [68] UiO-66 [115,117,119] with PIZOF-2 [113] and DUT-67 [119]. A detailed comparison of water-vapor adsorption isotherms for Zr-series-based MOFs is provided in Fig. 4(b). UiO-66 shown water-vapor uptake of 525 cm^3/g at a relative pressure of 0.90 and temperature of 293 K. However, UiO-66 did not possess cyclic stability; hence, it was not suitable for cyclic use applications. On the other hand, MOF-801 and MOF-841 exhibited good water-vapor adsorption uptake with cyclic stability. These adsorbents could exhibit the same adsorption uptake for many cycles, and thereby MOF-801 was found more promising adsorbent for cooling application [82].

In addition to MIL and Zr-series, many other hydrophilic MOFs were investigated in the literature, as summarized in Fig. 4(c). In a study [53], CPO-27 with nickel (Ni) metal node possessed a high attraction for water-vapors. The D-A equation was used to fit the adsorption equilibrium data [49,50,52,53]. The D-A model equations are provided in Table 2, whereas the corresponding values for the optimized parameters are exhibited in Table 3.

Fig. 4(c) shows that type-I adsorption isotherm can be seen with maximum uptake of 0.45 kg/kg at a relative pressure of 0.90 and a temperature of 25 °C. The CPO-27 possessed cyclic stability for adsorption uptake even after 50 adsorption/desorption cycles [53]. Water-vapor adsorption equilibrium for HKUST-1 and Fe-BTC has been experimentally investigated in the literature [55]. Langmuir and Sip equations were used to model adsorption equilibrium data. HKUST-1 showed type-1 adsorption isotherm and maximum uptake of 0.60 kg/kg at a relative pressure of 0.90, thereby finding a more suitable adsorbent [37]. In another study [106], Dual-Sided Langmuir-Freundlich (DSLF) equation (Table 2) was used to fit water-vapor adsorption data for HKUST-1. However, Fe-BTC showed type-III adsorption isotherm with a maximum uptake of 0.36 kg/kg at a relative pressure of 0.90. The optimized parameters for all models and all studied adsorbents are provided in Table 3.

Some of the MOFs reported in literature did not show good water-vapor adsorption uptake e.g. Birm-1 [55], Birm-1-K [55], Birm-1-Li [55], MOF-5 [62] and MOF-14 [105]. However, they performed better for other applications like gas separation.

3. Applications of MOF/water pairs

In recent decade, the MOFs adsorbents are extensively investigated for the development of open and close-cycle adsorption applications. Water is a typical adsorbate in case of open-cycle system application [60,89,91–93,133], whereas, ethanol [75–77], methanol [73] and water [49,50,52,53,55,67,72,81,83,97,99,134] are studied for closed-cycle system applications. Detail of applications is summarized in Fig. 5.

3.1. Adsorption cooling

Adsorption cooling systems are mainly closed-cycle systems consisted of an evaporator, adsorption beds, expansion valve, condenser, and associated accessories. Fig. 6 (a,b) shows a typical schematic

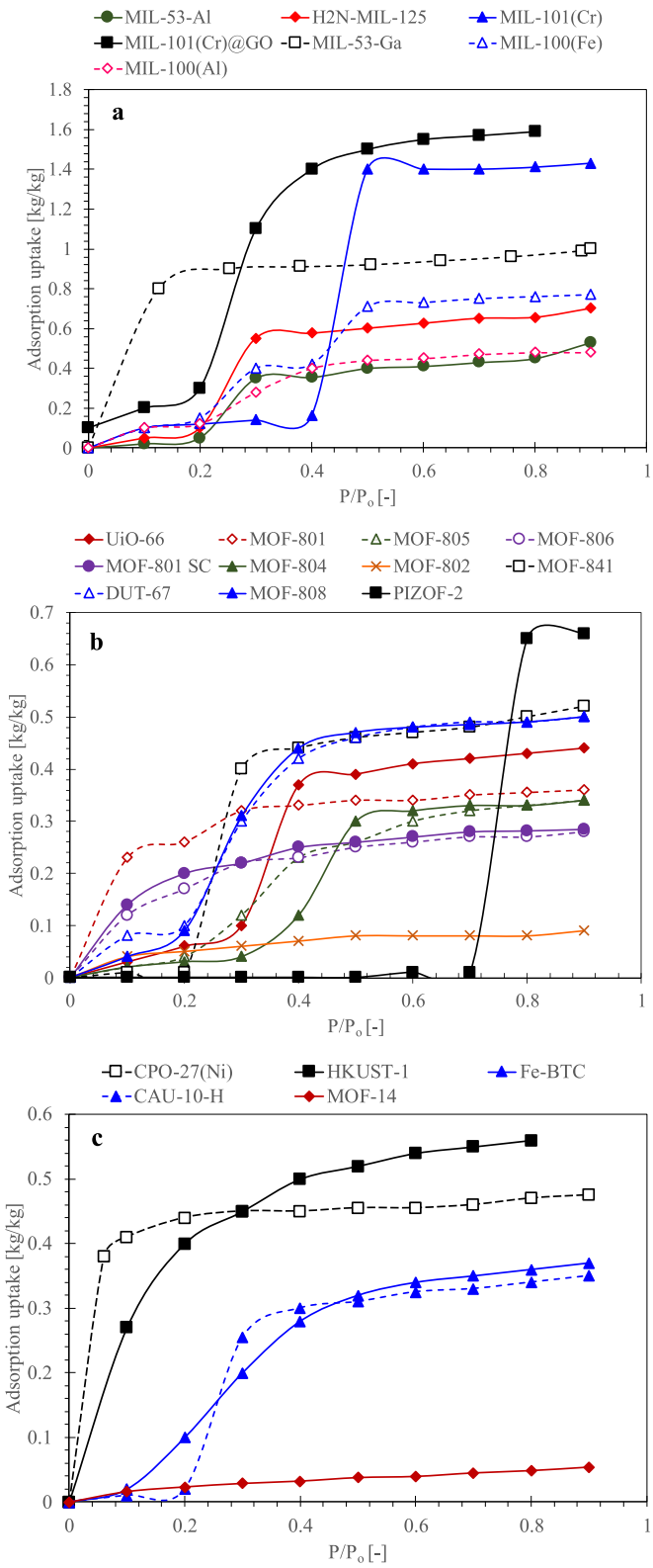

Fig. 4. Water-vapor adsorption isotherms for (a) MIL series-based MOFs, (b) zirconium-based MOFs, and (c) other MOFs available in the literature.

diagram of a closed-cycle adsorption cooling system and a Pressure-Temperature-Concentration (P-T—W) diagram demonstrating the ideal thermodynamic cooling cycle. Various adsorption cooling technologies/systems based on different cooling cycles have been reported in the literature [135–142]. It has been found that the COP and SCP of the system are mainly affected by heating sources [143,144], adsorption equilibrium and adsorbent-adsorbate interaction [3,145–147]. In this regard, MOFs are investigated with various adsorbates, e.g. water [148], ethanol [149] and methanol for adsorption cooling applications. The MOFs showed high adsorption uptake, even at lower concentrations [150]. For example, MIL-101(Cr) shown maximum uptake of ethanol, methanol and water of 1.10 kg/kg [77], 1.20 kg/kg [73] and 1.45 kg/kg [49], respectively. The MIL-101(Cr)/ethanol pair has been experimentally investigated in literature for adsorption cooling [77] and refrigeration [75] applications. MIL-101(Cr) possessed a methanol uptake of 0.51 kg/kg, which is twice that of activated carbon (i.e. 0.234 kg/kg). Adsorption equilibrium and kinetics have been experimentally tested, and the results revealed, it could be a promising candidate for developing cooling devices [77]. In a study [75], MIL-101(Cr) showed adsorption ability for many adsorption-desorption cycles (stable after 60 cycles) as the reduction in BET surface area was only 3.30%. MIL-101(Cr)/ethanol is completely regenerated at 100 °C, a relatively low regeneration temperature than activated carbons. Similarly, MIL-101(Cr) and HKUST-1 were investigated for methanol adsorption update [73]. The results showed that MIL-101(Cr) has higher performance when desorption temperature is less than 353 K. However, HKUST-1 has higher performance when evaporator temperature is greater than −5 °C and outperformed compared to activated carbons.

Hydrophilic MOFs have been investigated in the literature for single and two beds adsorption-based air-conditioning and cooling systems. In a study [53], CPO-27(Ni) has been experimentally tested to develop a single-bed adsorption refrigeration system and simulated for two beds adsorption systems for automobile air-conditioning. This study also compared the performance of CPO-27(Ni), RD-2060 and SAPO-34 to select appropriate adsorbent with higher COP and SCP values. Results have shown that CPO-27(Ni) has good performance with SCP values ranging from 80 W/kg to 105 W/kg. However, SAPO-34 outperformed both cases with the SCP value of 440 W/kg and a regeneration temperature of 130 °C, which is quite higher than CPO-27(Ni). There is an effect of condenser and evaporator temperature on SCP and COP of the system. In a study [49], CPO-27(Ni) was investigated for adsorption heat pump applications where it was best operated at low evaporator temperature (< 5 °C). Similarly, HKUST-1 and seven more MOFs [55] were investigated for adsorption chiller applications. The results showed that HKUST-1 has higher performance at lower evaporator temperature (< 5 °C) and 185% more water-vapor uptake than silica-gel.

However, not all the MOFs need to require low evaporator temperature for good performance, e.g. AlFs requires a high evaporator temperature of 20 °C [49]. In the case of the adsorption heat pump, the useful energy is heat used by the evaporator, condenser and adsorption beds/wheel. COP_h can be calculated by Eq. 1 [49].

$$COP_h = \frac{Q_{ads} + Q_e}{Q_{des}} \tag{1}$$

For an adsorption chiller, the evaporator energy is the useful energy from the device. COP_{ref} is calculated by Eq. 2.

$$COP_{ref} = \frac{Q_e}{Q_{des}} \tag{2}$$

The effect of regeneration temperature for CPO-27(Ni) and aluminium fumarate is shown in Fig. 7. It can be observed that COP_h and COP_{ref} of aluminium fumarate remain constant after 75 °C. However, in the case of CPO-27(Ni), it continuously increases up to 90 °C then becomes constant up to 115 °C. In another study [71], MIL-125-H_2N finds a promising candidate with SCP values ranging from 0.4–2.8 kW/kg with high cyclic and hydrothermal stability and low regeneration temperature. The feasibility of different hydrophilic MOFs and their use for closed-cycle applications is given in Table 4.

Table 2
Fundamental equations of the adsorption equilibrium models used in the literature for fitting of adsorption isotherms data of various MOF/water pairs.

Adsorption equilibrium model	Governing equation(s) of the model	MOFs
D-A equation	$w = w^{\circ} exp\left(-\left(\frac{A}{E}\right)^{n}\right)$ $A = R\,Tln\left(\frac{P}{P_o}\right)$	CPO-27 (Ni) [49,50,53] MIL-101(Cr) [50] Aluminium fumarate [50]
Dual-site Langmuir-Freundlich equation	$w = w_{m1}\frac{b_{DSLF1}P^{1/n_{DSLF1}}}{1+b_{DSLF1}P^{1/n_{DSLF1}}} + w_{m2}\frac{b_{DSLF2}P^{1/n_{DSLF2}}}{1+b_{DSLF2}P^{1/n_{DSLF2}}}$	HKUST-1 [106]
Langmuir equation	$w = \lfloor w^{\circ}\left[b.\left(P_{sat,T_{ref}}/P_{sat,T_{abs}}\right)\left(1+b.\left(P_{sat,T_{ref}}/P_{sat,T_{abs}}\right)\right)\right]\rfloor$ $w = w^{\circ}\frac{b\left(\frac{P}{P_o}\right)}{1+b\left(\frac{P}{P_o}\right)}$	HKUST-1 [55]
Freundlich equation	$w = H\left(\frac{P}{P_o}\right)^{1/m}$	MIL-101 (GO) [60]
Sip equation	$w = w^{\circ}\frac{b\left(\frac{P}{Po}\right)^{1/n}}{1+b\left(\frac{P}{P_o}\right)^{1/n}}$	MIL-101 (GO) [60] Fe-BTC [55]

Table 3
Optimized fitting parameters of the adsorption equilibrium models used in the literature for fitting of adsorption isotherms data of various MOF/water pairs.

Adsorption equilibrium model	MOFs	Optimized parameters of the models	Temperature [°C]	References
D-A equation	CPO-27 (Ni)	$n = 4$ $E = 10{,}014$ J/mol $w^{\circ} = 0.462$ kg//kg	25	[49] [52]
	MIL-101 (Cr)	$w = 0.42434\ exp\ (-0.0002825A)$ for $\frac{P}{P_{\circ}} \le 0.15$ $w = 0.4636 - 0.00024A + 5.4E-08A^2 - 4.06E-12A^3$ for $0.15 < \frac{P}{P_{\circ}} \le 0.4$ $w = 1.51 - \left(\frac{A}{1.35*T}\right)$ for $0.4 < \frac{P}{P_{\circ}} \le 0.5$ $w = 1.51 - 0.000266A + 0.363E - 6A^2 - 0.177E - 9A^3$ for $\frac{P}{P_{\circ}} > 0.5$	15–45	[50]
	Aluminium Fumarate	$w = 0.111993\ exp\ (-0.000258797A)$ for $A > 3987$ $w = 2.36129 - 9.93768E-04A + 1.05709E-07A^2$ for $2900 \le A \le 3987$ $w = -3.124455E-11A^3 + 1.68302E-07A^2 - 3.12E-04A + 0.5948$ for $A < 2900$	25	[50]
Freundlich equation	MIL-101 GO	$H = 0.59$ kg/kg; $m = 1.2$ for $\left(\frac{P}{P_{\circ}} \le 0.35\right)$	25	[60]
Dual site Langmuir-Freundlich Equation	HKUST-1	Temperature (K) / w_{m1} (mmol/g) / b_{DSLF1} ($mbar^{1/n}$) / $1/n_{DSLF1}$ / w_{m2} (mmol/g) / b_{DSLF2} ($mbar^{1/n}$) / $1/n_{DSLF}$ 288 / 22.54 / 0.385 / 0.656 / 10.63 / 1.037×10^{-14} / 0.0813 298 / 20.77 / 0.11 / 0.569 / 11.51 / 0.102×10^{-17} / 0.0849 308 / 17.38 / 0.0253 / 0.478 / 13.82 / 2.015×10^{-14} / 0.1202 318 / 14.65 / 0.0045 / 0.428 / 16.52 / 2.658×10^{-18} / −0.1635	15–45	[106]
Sip equation	Fe-BTC	$w^{\circ} = 0.38$ kg//kg $b = 2.75$ $n = 3.63$	52	[55]
	MIL-101 GO	$w^{\circ} = 1.55$ kg//kg $b = 4.48 \times 10^3$ $n = 0.0847$ for $\frac{P}{P_o} \ge 0.35$	25	[60]
Langmuir equation	HKUST-1	$w^{\circ} = 0.64$ kg//kg $b = 8.33$	52	[55]

3.2. Desiccant air-conditioning

The desiccant air-conditioning (DAC) system usually consists of a desiccant unit (wheel/rotor or block type), heat exchanger, heating source, a low-cost cooling source, and some associated accessories [151]. A typical schematic diagram of a DAC system and the corresponding psychrometric representation of the DAC cycle are shown in Fig. 8(a) and (b). In a study [60], MIL-101(Cr)@GO has simulated for adsorption air-conditioning open-cycle system and results were compared with conventionally used silica-gel based system. Different parameters were investigated, e.g. rotational speed, cooling energy consumption, thermal energy consumption, energy, environmental and

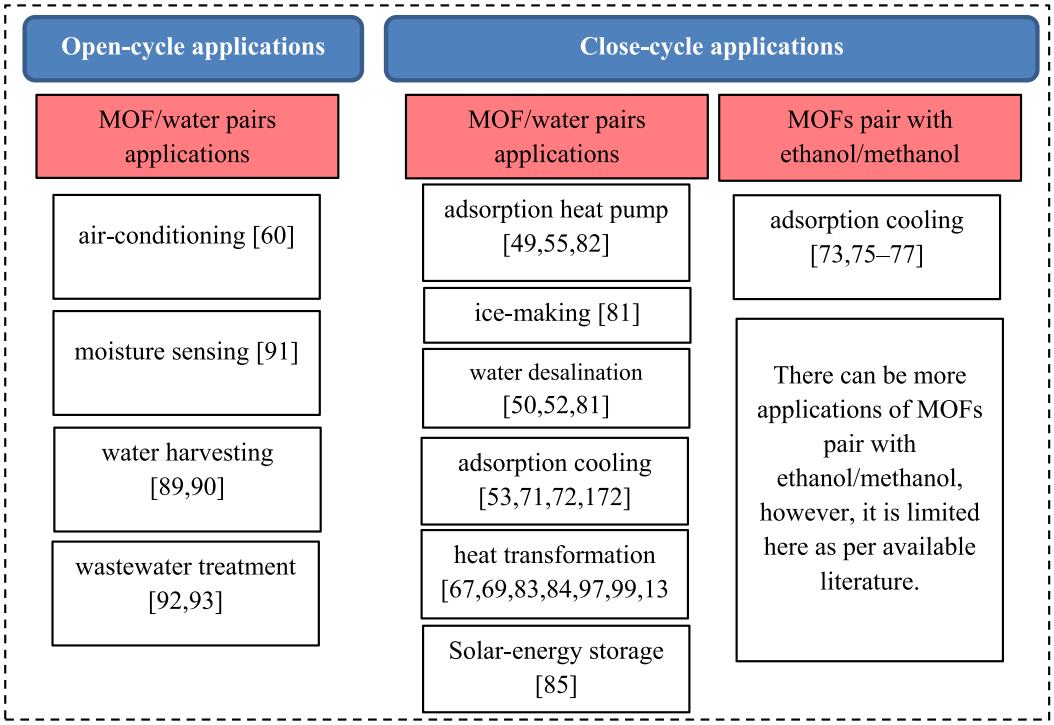

Fig. 5. Insights of applications of MOF adsorbents studied in the literature.

economic analysis and dehumidification efficiency of the desiccant wheel (DW). Dehumidification effectiveness (DE) is calculated by Eq. 3 [60].

$$\eta_{deh} = \frac{W_{pro,in} - W_{pro,out}}{W_{pro,in}} = 1 - \frac{W_{pro,out}}{W_{pro,in}} \tag{3}$$

Dehumidification effectiveness was taken as a function of the process air RH. Dehumidification effectiveness increases when temperature and RH of inlet air increases, as shown in Fig. 9. The DE of MIL-101(Cr) is higher than silica-gel; this is because of the high uptake of MIL-101(Cr).

In another study [152], a solar-driven HKUST-1 based DAC system was simulated. A comparison between silica-gel (type B) coated heat exchanger (SCHE), and MOFs coated heat exchanger (MCHE) at different outlet temperatures had made. The MCHE has 1.28 times more dehumidification capacity than SCHE when cycle time 120 s, as shown in Fig. 10. The dehumidification capacity of MCHE rises with an increase in regeneration temperature at a cooling water temperature range of 25 °C and 30 °C. In SCHE, the increase in dehumidification capacity is very low, with an increase in regeneration temperature. MCHE was found to be more applicable for a shorter cycle time than SCHE due to the low water holding capacity of HKUST-1.

3.3. Water harvesting and desalination

Water harvesting can be a promising application of the MOFs as they can adsorb water at low concentration, and desorption occurs at relatively low temperature [133]. A Zr-based water harvesting device for arid climate has been designed and investigated in a study, as shown in Fig. 11 [89]. It is estimated that currently, 150 countries are producing desalination water of about 30 billion m^3/year by operating 18,000 desalination plants [153,154]. Many studies have been reported in the literature in which silica-gel and other conventional adsorbent have successfully investigated for single−/ two-bed adsorption desalination systems [155–166]. However, the MOFs have been utilized for water desalination application and freshwater production, ice and some amount of cooling. In another study [52], CPO-27(Ni) has experientially investigated water desalination for a one-bed adsorption-based desalination system. A schematic diagram of the single bed of adsorption-based desalination system is shown in Fig. 12. The performance of the water desalination system is assessed on the specific daily water production (SDWP), which can be calculated by using Eq. 4 [52].

$$SDWP = \int_0^{t_{cycle}} \frac{Q_{cond.}\tau}{h_{fg}M_a} dt \tag{4}$$

The SDWP of the system was affected by desorption and the condenser temperature, the effect of regeneration temperature on the SDWP is shown in Fig. 13. SDWP at different condenser and regeneration temperature reproduced from [52]. It can be observed that most of the MOFs shown good results when operated at low condenser temperature, e.g. CPO-27(Ni) has maximum water production of 22.8m^3/tone. ads/day and producing cooling of 219.9 Rton/t when operated at maximum inlet condenser temperature of 5 °C and inlet evaporator temperature of 40 °C. Therefore, reducing the condenser temperature and increasing the evaporator temperature results in maximum water production and increased cooling capacity. In another study [50], three MOFs, CPO-27(Ni), MIL-101(Cr) and aluminium fumarate (AlFs) have investigated for two beds adsorption-based desalination systems. CPO-27(Ni) gave maximum water production at low condenser temperature and high evaporator temperature with a regeneration temperature of ≥110 °C. Similarly, AlFs performed better at a high evaporator temperature of 20 °C with water production of 6.3 m^3/ton.day. However, it required a low regeneration temperature of 70 °C. In this regard, MIL-101(Cr) performed good and shown exceptional results with maximum water production of 11 m^3/ton.day.

CPO-27(Ni) is the best candidate for adsorption-based desalination system because of its shape of adsorption isotherm and maintains its

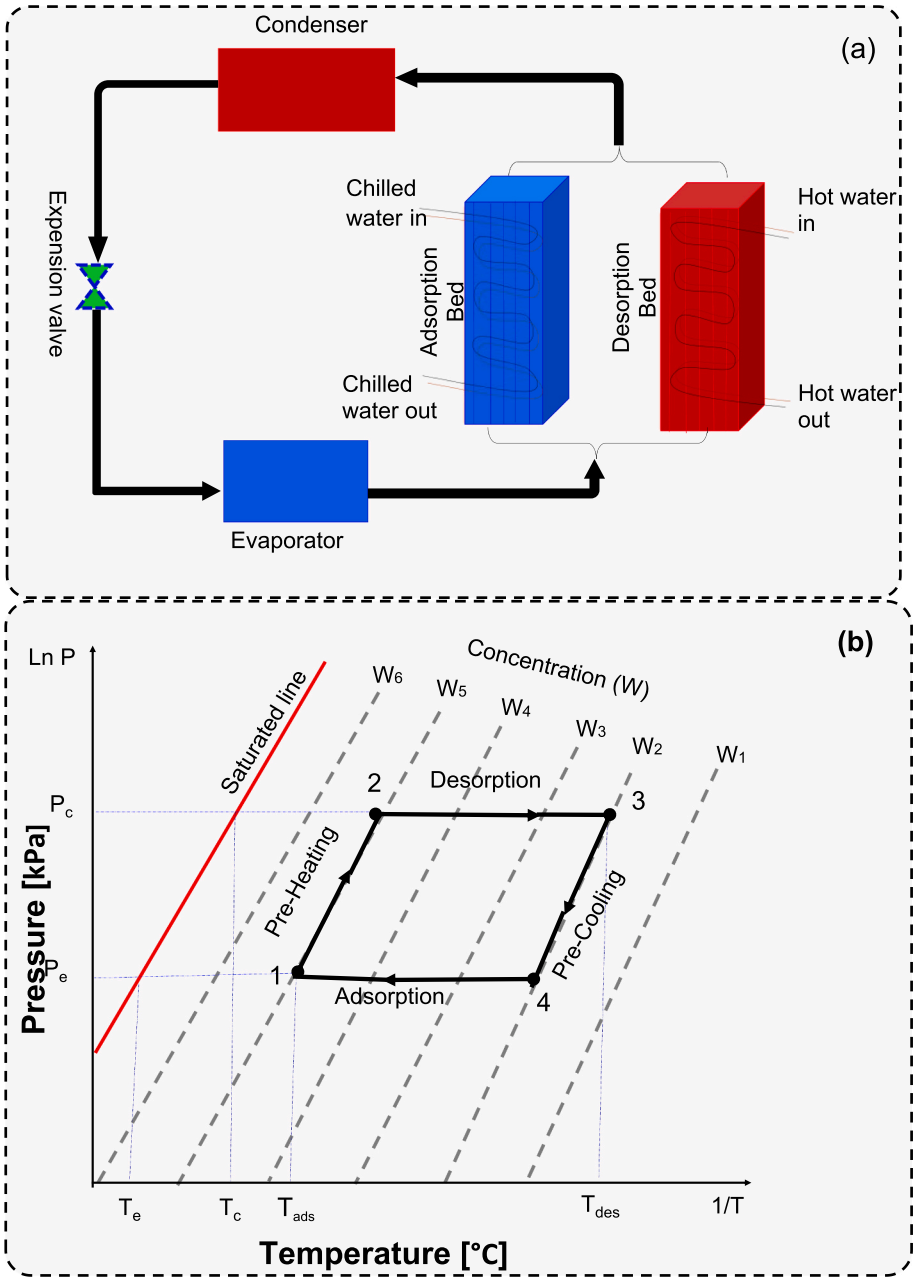

Fig. 6. (a) Schematic diagram of the adsorption cooling system, and (b) P-T-W diagram of the adsorption cooling cycle.

adsorption capacity when the relative pressure ratio is maintaining. In another study [81], water desalination systems combined with ice-making with one-bed adsorption system have been experimentally investigated. A schematic diagram of water desalination combined with an ice-making system is shown in Fig. 12(b). CPO-27(Ni) used to obtain maximum water and ice production is 1.8 ton/day/ton-ads and 8.3 ton/day/ton-ads, respectively, to achieve a low evaporator temperature of 5 °C. The applicability of different hydrophilic MOFs for various applications is given in Table 5.

4. Prospects of MOFs adsorption systems and barrier in the commercialization

Although the adsorption phenomenon is well-known for centuries, however, considering this conception for cooling, air-conditioning and water desalination applications is started in the twentieth century to replace environmentally harmful compressor-based systems. From that moment, researchers worldwide are working to develop energy-efficient adsorption-based technologies/systems. In this regard, their research's key focus is to develop optimum adsorbent materials by which the overall efficiency/performance of the adsorption systems can be improved. The optimum material should have the ability to adsorb a larger amount of adsorbate for a wide range of system applications. The MOFs are a new class of micro- and nano-porous group of adsorbents with exclusive adsorption and physical properties. Recently, MOFs have been extensively investigated for the development of such systems. Fig. 14 shows a comparison between the studied five groups of hydrophilic MOFs. It was found that MIL series-based MOF have greater potential in various water adsorption and air-conditioning applications due to their stable structure and higher adsorption uptake. On the other

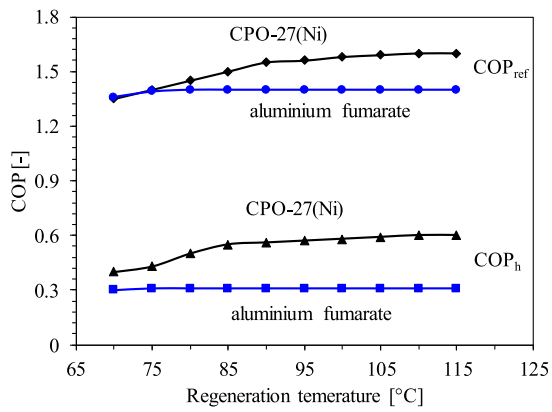

Fig. 7. Effect of regeneration temperature on COP at T_{con} = 35 °C and T_{eva} = 5 °C reproduced from [49].

hand, Cu-based MOFs perform better at relatively low-pressure and are highly dependent on pressure changes. Besides, Cu—Cu bond length elongates in the presence of moisture, increasing the moisture stability of this group in lower pressure ranges.

A state-of-the-art comparison of COP between the MOFs and conventional adsorbents-based cooling systems is developed in Fig. 15 from 1975 to 2020. The adsorbents used for this comparison are reffered from following studies [8,10,17–19,27,28,34,37,41,49,70,74,78,87,88,129,135–144,147–151,157,158,168–172]. The conventional adsorbents-based systems are only able to achieve a COP level of 0.85 since 1975. However, the majority of the MOFs based systems provide considerably higher performance as compared to conventional adsorbent based systems. The main bottleneck in the lower COP level is the low adsorption equilibrium amount. It has been found that conventional adsorbents possess low water-vapor uptake, which results in low system performance and high system size. The MOFs exhibit 2 to 3 times higher water-vapor adsorption uptake as compare to conventional silica-gel. Some of the MOFs result in adsorption uptake of 1.45 kg/kg, which can be

Table 4
Applications of the hydrophilic MOFs considered in the literature using close-cycle systems.

MOFs	Methodology used	Application(s)	Regeneration temperature [°C]	Condenser temperature [°C]	Evaporator temperature [°C]	Findings and conclusion	Reference
CPO-27(Ni)	Modeling	Adsorption heat pumps	≥90	30–45	5	• High regeneration temperature greater than 90 °C • Low evaporator temperature	[49]
	Dynamic modeling + experiment + Simulation	Automotive air-conditioning	≥90 and up to 130	15–35	5–25	• Single and two-beds air-conditioning system and COP value is 0.3 • SCP = 80–105 W/kg • Two beds adsorption cooling system has cooling capacity and SCP values of 2.4 kW and 400 W/kg, respectively, at cycle time of 900 s and desorption temperature of 130 °C	[53]
Aluminium fumarate	Modeling	Adsorption heat pump	70	40–45	20	Suitable for • Low regeneration temperature less than or equal to 70 °C • High evaporator temperature greater than 20 °C	[49]
NH_2-MIL-125	Experiment + dynamic modeling	Adsorptive cooling	90	N/A	N/A	Suitable for • High COP at low desorption/ regeneration temperature • SCP = 0.4–2.8 kW/kg • High hydrothermal stability	[71]
HKUST-1	Experiment + analysis	Adsorption chiller	85	32	5	Suitable for • More uptake 185.7% compared to silica-gel at evaporator temperature 5 °C • Low evaporator temperature of 5 °C	[55]
Triazolyl phosphonate MOF	Modeling/ simulation	Adsorptive cooling	110	N/A	N/A	Suitable for • Regeneration temperature higher than 110 °C is not meaningful so operating on low regeneration temperature. • Higher performance than zeolite	[72]
Fe-BTC	Experiment	Adsorption chiller	85	32	12	Suitable for • Cascade cooling • High performance at high evaporator temperature greater than 10 °C	[55]
MOF-801	Experiment	Adsorption cooling	80–85	30	5	• High performance with COP is 0.67 and SCP is 0.29 ± 0.01 Kw/kg • Isosteric heat of adsorption 55 to 60 kJ/ mol in the uptake range 0.05–0.35 kg/kg	[82]
MIL-100(Fe)	Experiment	Adsorption cooling	95	20	N/A	Suitable for • Energy storage density is 1200 Wh/kg and COP is 0.8 with cycle time of 90 mint • It produced cooling effect of 337 W/kg	[129]

Key: N/A: not available.

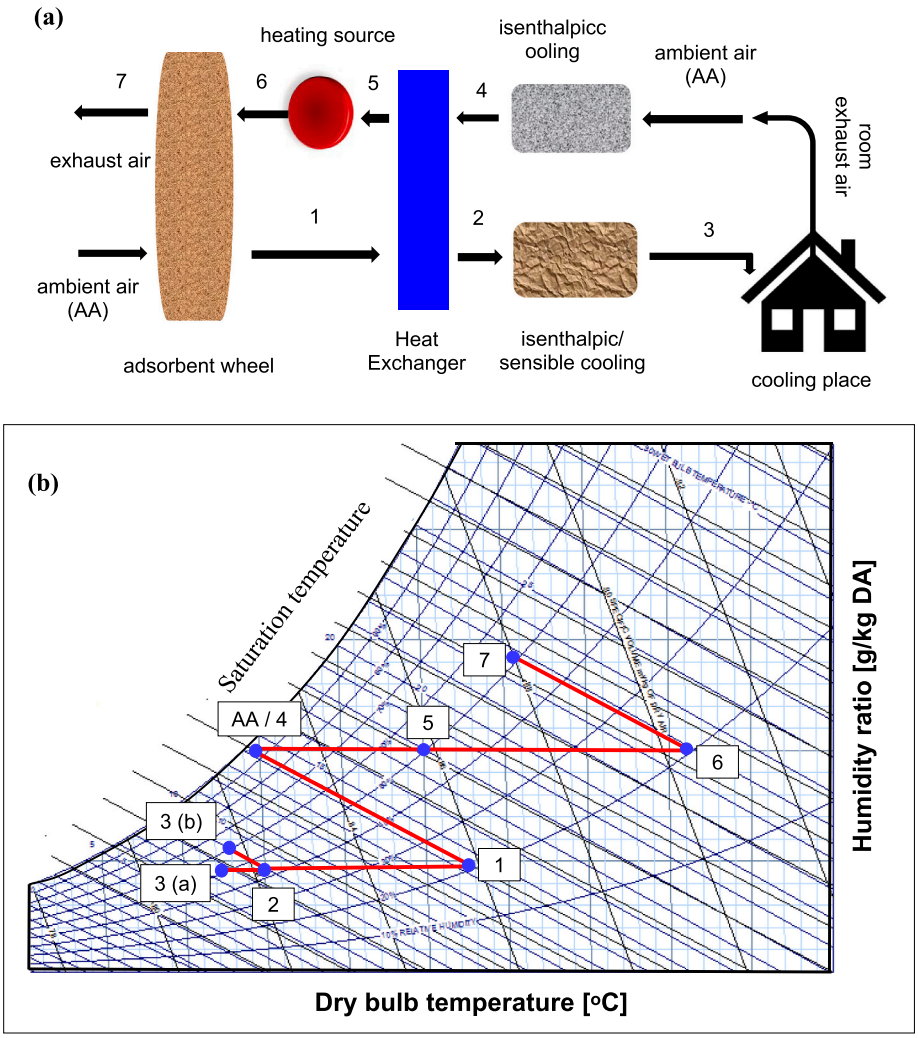

Fig. 8. (a) Schematic diagram of the desiccant air-conditioning system and (b) Psychrometric representation of the desiccant air-conditioning cycle.

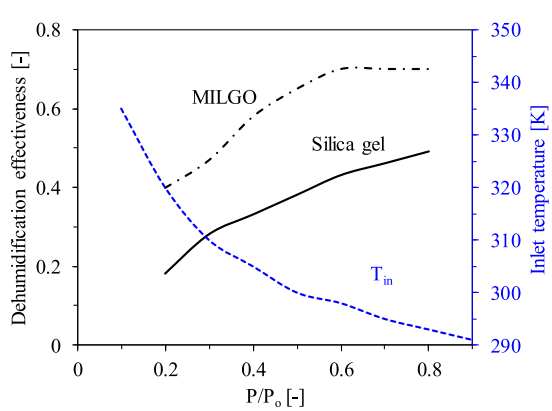

Fig. 9. Comparison of dehumidification effectiveness by silica-gel as a function of relative pressure of process air of MOF based adsorbents (for process absolute air humidity of 0.01 kg/kg and desorption temperature of 333 K [60].

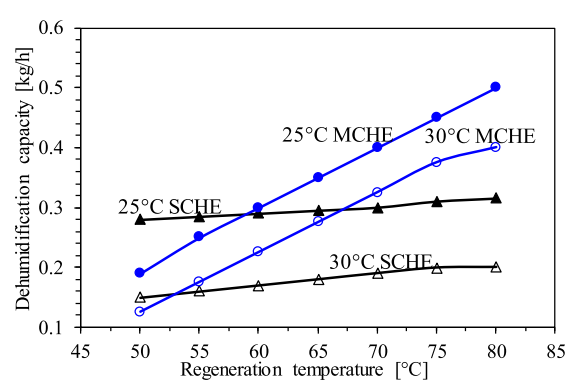

Fig. 10. Dehumidification capacity of MCHE and SCHE systems at cooling water temperatures of 25 °C and 30 °C [152].

increased to 1.60 kg/kg by coating techniques. Therefore, this review is aimed to provide comprehensive detail of water-vapor adsorption uptake by the hydrophilic MOF adsorbents available in the literature. The development of high adsorbate uptake MOF materials helps to overcome the limitations of conventional adsorbent systems, and the COP level is improved to almost 2. Similarly, the dehumidification capacity of the MOF coated heat exchanger is found 1.28 times higher compared to the silica-gel coated heat exchanger. The MOFs produce maximum desalination water of 25.5 m^3/ton.day, which is higher than silica-gel (i.e. 13.5 m^3/ton.day). The energy consumption and environmental/economic analyses conducted in the literature show that the MOF systems are a better option than conventional systems.

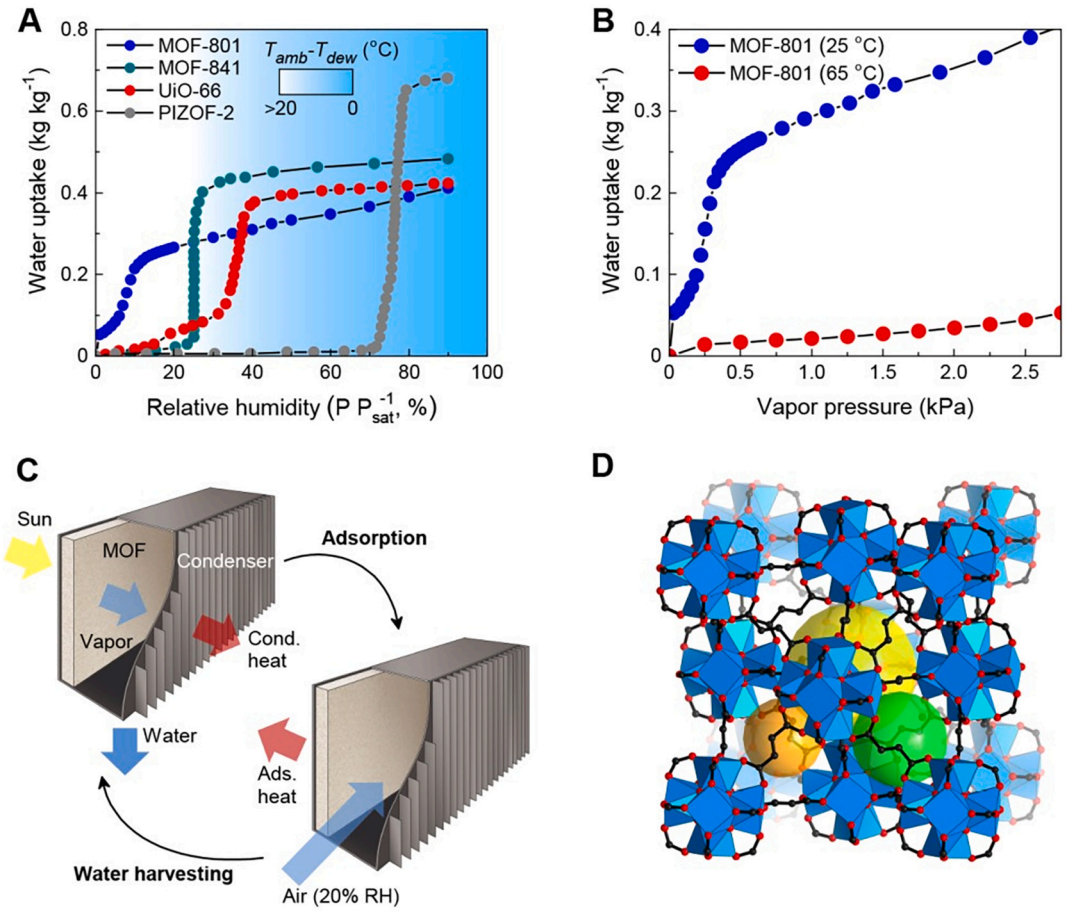

Fig. 11. MOF based water harvesting device driven by natural sunlight [89].

Based on crystal, structural properties and water-vapor adsorption equilibrium amount, it can be summarized that the development of advance MOFs is strengthening the desperate attempts to develop energy-efficient and high-performance adsorption systems. The MOF adsorption systems are coming strongly to the commercial market and we may soon see one of these systems sold commercially. However, a lots of future works are needed to commercialize them accordingly and to replace the traditional technologies. Considering the above-mentioned prospectus of the MOF adsorbents/systems, the recommended future works include: (i) Developing the optimum MOF adsorbents with sophisticated thermo-physical properties including pore volume, surface area, thermal conductivity, and crystal structure etc. (ii) Characterizing, measurement and treatments of adsorbent-adsorbate pairs for the development of advance adsorption capacities (including adsorption equilibrium, adsorption kinetics, and adsorption heat) for various heat transformation applications, (iii) Integration of advance MOFs in adsorption systems for establishment of multi-bed and/or multi-stage strategies, and (iv) Optimizing operating parameters of the adsorption systems depending upon the available waste heat and/or renewable energy options.

5. Conclusions

Metal-organic frameworks (MOFs) or porous coordination polymers are a highly porous class of adsorbents with excellent structural and water-vapor adsorptive properties. These are new micro to nano porous class of adsorbent with great potential to develop energy-efficient thermally driven adsorption systems/technologies. The hydrophilic MOF adsorbents are critically studied in the literature for the development of various adsorption-based applications. Thereby, this study provides a comprehensive review of various hydrophilic MOF adsorbents concerning crystal formation, structural stability, water-vapor adsorption equilibrium, adsorption chemistry, and associated potential applications, i.e. cooling, air-conditioning, and water distillation/harvesting. Furthermore, a comprehensive comparison of the coefficient of performance between the studied MOFs and conventional adsorbents is developed for the years 1975 to 2020. It has been found that the majority of the MOFs based adsorption systems provide considerably higher performance as compared to most of the conventional adsorbents-based systems. The study concludes that the MOF based systems are coming strongly to the commercial market, and we may soon see one of these systems sold commercially. The insights of the conclusions are as follows:

Zinc-based MOFs are not stable in the presence of water-vapors due to Zn metal's sensitivity to water molecules, e.g. MOF-5 is not stable when water contents are more than 4%. Zirconium-based MOFs are found relatively more stable in the presence of water-vapors; however, adsorption uptake for most of the adsorbents of this category is quite low. In this regard, UiO-66 with micropores possesses water-vapor adsorption uptake of 0.4 kg/kg at 25 °C and saturation condition. However, it has no cyclic stability, and the adsorption ability is perceptibly reduced after continuous cyclic use, limiting its usage. On the other hand, MOF-801 and MOF-841 show maximum uptake of 0.32 kg/kg and 0.53 kg/kg, respectively, at 25 °C (saturation condition). The

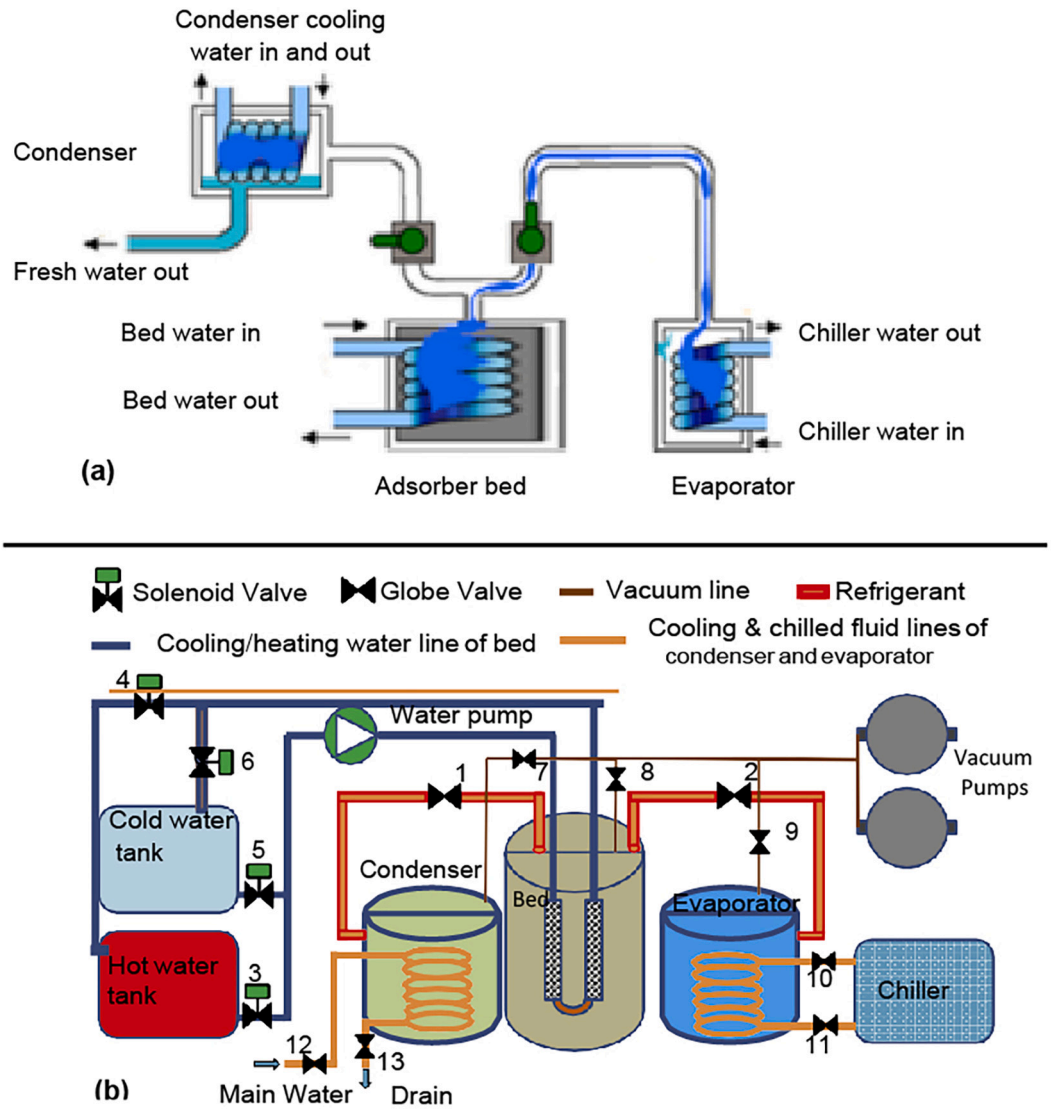

Fig. 12. Schematic diagram of (a) single bed water desalination system [52] and (b) one be adsorption based water desalination and ice-making system [81].

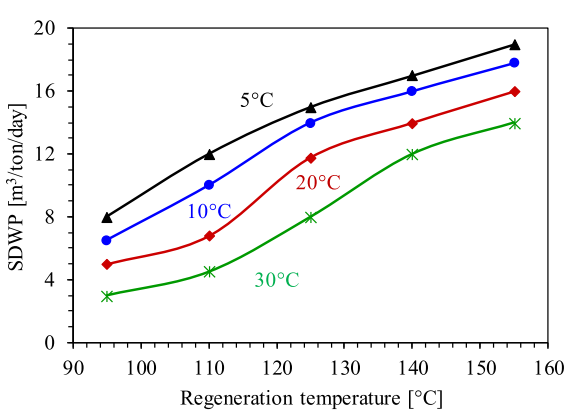

Fig. 13. SDWP at different condenser and regeneration temperature reproduced from [52].

MOF-801 is found a promising candidate for air-conditioning application due to cyclic stability. It also shows good results for water harvesting application with maximum water production of 0.19 L/kg (considering kinetics losses) at a relative humidity of 40% and a regeneration temperature of 85 °C. Nickle-based CPO-27 is found stable in the presence of water-vapors and provides type-I adsorption isotherm according to IUPAC classification with the uptake of 0.47 kg/kg (at saturation). It possesses cyclic stability and gives COP of 0.45 for automotive air-conditioning application. It provides specific daily water production of 22.8 m^3/t.ads/day and cooling effect of 215.99 Rton/t in case of water desalination application for inlet temperature of 40 °C (condenser) and 5 °C (evaporator). Copper-based HKUST-1 results adsorption uptake of 0.55 kg/kg at 25 °C (saturation condition). It is a promising candidate for air-conditioning application, whereas its stability reduces at a high relative pressure range due to Cu—Cu bond length elongation.

On the other hand, MIL series-based MOFs possess stable structures and exhibit adsorption isotherms of type-IV and type-V. In this regard, MIL-101(Cr) possesses the highest water-vapor adsorption uptake (i.e. 1.45 kg/kg at 25 °C on saturation condition) compared to the studied MOFs. Based on the reported results, it performed better in air-conditioning, single−/ two-bed desalination and heat transformation applications/systems. It also shows good performance with different refrigerants other than water, e.g. ethanol and methanol. Besides, adsorption uptake can also increase from 1.45 to 1.6 kg/kg when coated with graphite oxide. Similarly, MIL-53(Al) exhibits specific daily water production of 25.5 m^3/ton.day (maximum) with a specific cooling

Table 5
Applications of the hydrophilic MOFs considered in the literature using open-cycle systems.

MOFs	Methodology used	Application(s)	Regeneration temperature [°C]	Condenser temperature [°C]	Evaporator temperature [°C]	References
OPEN-CYCLE SYSTEMS						
MIL-101(Cr)@GO	Simulation + case study	Air-conditioning	50–70	N/A	N/A	[60]
Findings and conclusion						
• The dehumidification efficiency of MIL-101(Cr)@GO is higher than silica-gel • The rotational speed of MIL-101(Cr)@GO is significantly higher than silica-gel as high water-vapor uptake the optimal speed is 40 rev/h • Thermal energy consumption for the regeneration of DW is 40% lower than silica-gel, resulting in a reduction in cooling energy consumption about 11% than silica-gel • Energy, environment and economic analysis showed that MIL-101(Cr)@GO based DW has significant improvements than silica-gel based DW						
HKUST-1	Simulation	Desiccant cooling	80	N/A	N/A	[152]
Findings and conclusion						
• Dehumidification capacity of MCHE is 1.28 times higher than SCHE when cycle time 120 s • The dehumidification capacity of MCHE is higher than SCHE when cycle time is shorter and cooling water temperature is high approximately equal to 80 °C for long time period more than 240 s SCHE performance is good as compare to MCHE • HKUST-1 has good performance when cycle time is 120 s and cooling water temperature is 80 °C						
PHCM-MOF	Simulation	Humidity control	≥40	N/A	N/A	[86]
Findings and conclusion						
• Maximum water-vapor adsorption uptake of 1.63 kg/kg at RH of 80% and temperature of 25 °C with S shape of adsorption isotherm • Adsorption occurs when RH is higher than 40% and desorption start when RH reduce to 45%						
WATER HARVESTING AND DESALINATION SYSTEMS						
MOF-801	Experiment	Water harvesting	≥85	33	N/A	[89,133]
Findings and conclusions						
• The total amount of harvested water is predicted at the end of all adsorption and desorption cycles in a day. It can harvest water about 0.19 L/kg of MOF after overcoming all kinetics limitations. • Predicted water harvesting ability which is 0.28 L/kg at condenser temperature of 33 °C and absorber temperature of 100 °C • Experimental water production is 0.21 L of water per kg of MOF at RH 40% for a single cycle which is nearly same as predicted water production • Harvested water has good quality as MOF-801 has higher hydrothermal stability and zirconium metal is stable in presence of water • MOF-801 is a promising candidate to work at low RH ranging from 15 to 20% at regeneration temperature is high 85 °C • MOF-801 has capacity to harvest water 2.8 L/kg of MOF daily at RH as low as 20% and no input of energy required						
CPO-27(Ni)	Experiment + numerical modeling, Experiment + simulation	Water desalination+ ice-making, water desalination cooling	≥110	40	5	[50,52,81]
Findings and conclusion						
• Sea water and fresh water used as refrigerant to achieve low evaporator temperature ≤ 0 °C • Production of ice = 8.3ton/day/ton-ads, COP of 0.9 and desalination of water of 1.8ton/day/ton-ads with optimum salinity is 35,000 ppm • Produce 5.4 times more SDWP with value of 8.9 ton/day/ton-ads using sea and fresh water as refrigerant as compare to ammonia used in conventional systems • Maximum water production = 22.8 m^3/t.ads/day, cooling = 215.99 Rton/t with condenser inlet temperature = 40 °C and evaporator inlet temperature = 5 °C						
Aluminium fumarate	Modeling	Water desalination	70–85	25	20	[50,129,167]
Findings and conclusions						
• It has SDWP and SCP of 6.30 m^3/ton.day and 21.2 Rton/t, respectively • In another study it has maximum SDWP 25.5 m^3/ton.day and SCP of 789.4 W/kg						
MI-L101 (Cr)	Modeling	Water desalination	N/A	N/A	N/A	[50]
Findings and conclusions						
• Outperform with maximum SDWP of 11m^3/ton.day						
MIL-100(Fe)	Experimental + modeling	Water desalination	95	20	N/A	[129]
Findings and conclusions						
• Maximum SDWP is 14 m^3/ton.day with moderate cooling effect, and without cooling effect its SDWP is 19 m^3/ton.day at high evaporator temperature						

Key: N/A: not available.

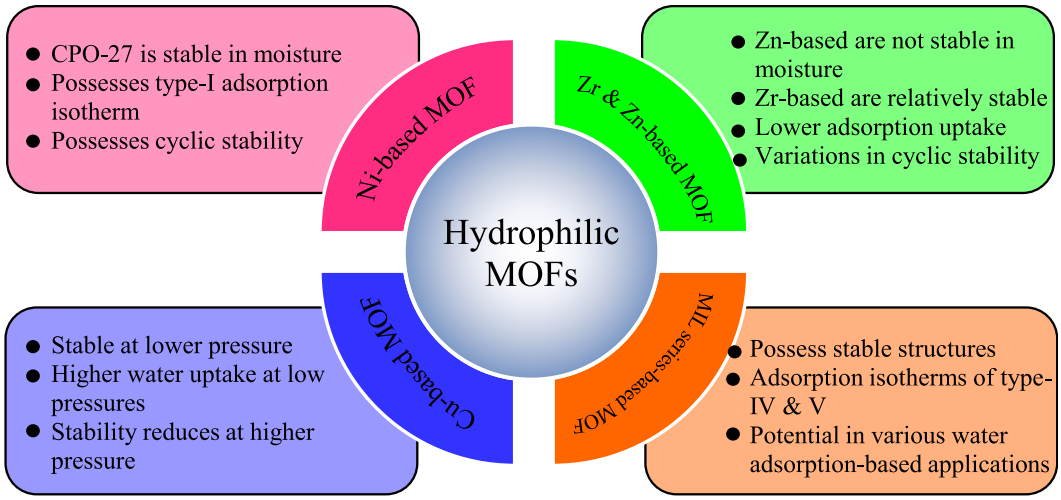

Fig. 14. A comparison of adsorption characteristics between the studied groups of hydrophilic MOFs, i.e. Ni-based, Cu-based, Zr-based, Zn-based and MIL series-based MOFs.

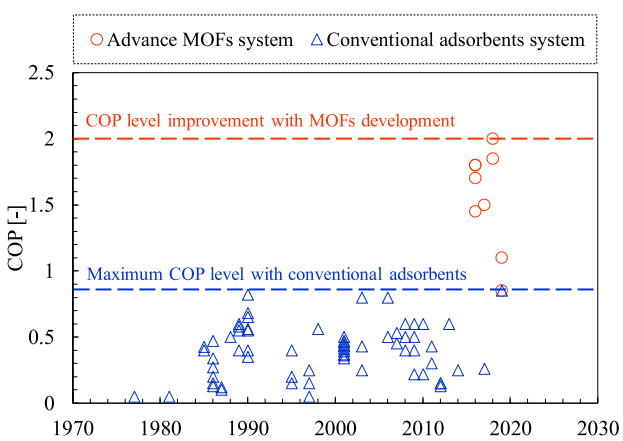

Fig. 15. COP trend of conventional adsorbent based cooling system and improvement with advance MOFs development. The adsorbents used for this comparison are referred from following studies [8,10,17–19,27,28,34,37,41,49,70,74,78,87,88,129,135–144,147–151,157,158,168–172].

power of 789.4 W/kg in water desalination application. It has been found that MIL-101(Cr) and MIL-53(Al) are promising hydrophilic MOFs which can be considered for various water adsorption-based applications.

Declaration of Competing Interest

The authors declare that they have no known competing financial interests or personal relationships that could have appeared to influence the work reported in this paper.

Acknowledgements

This research was carried out with the financially supported of Bahauddin Zakariya University, Multan-Pakistan under the Director Research/ ORIC grant entitled "Investigation of agriculture based low-cost ad/sorbents for desiccant air-conditioning applications" awarded to Principal Investigator Dr. Muhammad Sultan. The 2nd Author (Dr. Muhammad Sultan) gratefully acknowledges the support from the Canadian Queen Elizabeth II Diamond Jubilee Scholarships (QES). The QES is managed through a unique partnership of Universities Canada, the Rideau Hall Foundation (RHF), Community Foundations of Canada (CFC), and Canadian universities.

References

[1] M. Sultan, I.I. El-Sharkawy, T. Miyazaki, B.B. Saha, S. Koyama, An overview of solid desiccant dehumidification and air conditioning systems, Renew. Sust. Energ. Rev. 46 (2015) 16–29, https://doi.org/10.1016/j.rser.2015.02.038.
[2] B. Choudhury, B.B. Saha, P.K. Chatterjee, J.P. Sarkar, An overview of developments in adsorption refrigeration systems towards a sustainable way of cooling, Appl. Energy 104 (2013) 554–567, https://doi.org/10.1016/j.apenergy.2012.11.042.
[3] M.M. Younes, I.I. El-Sharkawy, A.E. Kabeel, B.B. Saha, A review on adsorbent-adsorbate pairs for cooling applications, Appl. Therm. Eng. 114 (2017) 394–414, https://doi.org/10.1016/j.applthermaleng.2016.11.138.
[4] Q.W. Pan, R.Z. Wang, Study on boundary conditions of adsorption heat pump systems using different working pairs for heating application, Energy Convers. Manag. 154 (2017) 322–335, https://doi.org/10.1016/j.enconman.2017.11.023.
[5] M. Sultan, T. Miyazaki, S. Koyama, Optimization of adsorption isotherm types for desiccant air-conditioning applications, Renew. Energy 121 (2018) 441–450, https://doi.org/10.1016/j.renene.2018.01.045.
[6] B.B. Saha, K. Uddin, A. Pal, K. Thu, Emerging sorption pairs for heat pump applications: an overview, JMST Adv. (2019), https://doi.org/10.1007/s42791-019-0010-4.
[7] Y. Jiang, M.H. Bagheri, R.T. Loibl, S.N. Schiffres, Thermodynamic limits of adsorption heat pumps: A facile method of comparing adsorption pairs, Appl. Therm. Eng. 160 (2019) 113906, https://doi.org/10.1016/j.applthermaleng.2019.113906.
[8] A. Sakoda, M. Suzuki, Simultaneous transport of heat and adsorbate in closed type adsorption cooling system utilizing solar heat, J. Sol. Energy Eng. Trans. ASME 108 (1986) 239–245, https://doi.org/10.1115/1.3268099.
[9] A.A. Askalany, M. Salem, I.M. Ismael, A.H.H. Ali, M.G. Morsy, B.B. Saha, An overview on adsorption pairs for cooling, Renew. Sust. Energ. Rev. 19 (2013) 565–572, https://doi.org/10.1016/j.rser.2012.11.037.
[10] R.E. Critoph, R. Vogel, Possible adsorption pairs for use in solar cooling, Int. J. Ambient Energy 7 (1986) 183–190, https://doi.org/10.1080/01430750.1986.9675500.
[11] M. Hamdy, A.A. Askalany, K. Harby, N. Kora, An overview on adsorption cooling systems powered by waste heat from internal combustion engine, Renew. Sust. Energ. Rev. 51 (2015) 1223–1234, https://doi.org/10.1016/j.rser.2015.07.056.
[12] A. Alahmer, S. Ajib, X. Wang, Comprehensive strategies for performance improvement of adsorption air conditioning systems: a review, Renew. Sust. Energ. Rev. 99 (2019) 138–158, https://doi.org/10.1016/j.rser.2018.10.004.
[13] M. Sultan, T. Miyazaki, B.B. Saha, S. Koyama, H.-S. Kil, K. Nakabayashi, et al., Adsorption of Difluoromethane (HFC-32) onto phenol resin based adsorbent: theory and experiments, Int. J. Heat Mass Transf. 127 (2018) 348–356, https://doi.org/10.1016/j.ijheatmasstransfer.2018.07.097.
[14] X. Zheng, T.S. Ge, R.Z. Wang, Recent progress on desiccant materials for solid desiccant cooling systems, Energy 74 (2014) 280–294, https://doi.org/10.1016/j.energy.2014.07.027.
[15] N. Asim, M.H. Amin, M.A. Alghoul, M. Badiei, M. Mohammad, S.S. Gasaymeh, et al., Key factors of desiccant-based cooling systems: materials, Appl. Therm. Eng. 159 (2019) 113946, https://doi.org/10.1016/j.applthermaleng.2019.113946.
[16] M.L. Elsayed, R.H. Mohammed, C. Chow L, Mesalhy O, Su M., Revisiting the adsorption equilibrium equations of silica-gel/water for adsorption cooling applications, Int. J. Refrig. 86 (2017) 40–47, https://doi.org/10.1016/j.ijrefrig.2017.10.038.
[17] E.C. Boelman, B.B. Saha, T. Kashiwagi, Experimental investigation of a silica gel-water adsorption refrigeration cycle-the influence of operating conditions on cooling output and COP, ASHRAE Transactions 101 (1995) 358–366.

[18] B.B. Saha, A. Akisawa, T. Kashiwagi, Silica gel water advanced adsorption refrigeration cycle, Energy 22 (1997) 437–447, https://doi.org/10.1016/S0360-5442(96)00102-8. Elsevier Ltd.

[19] R.E. Critoph, Activated carbon adsorption cycles for refrigeration and heat pumping, Carbon N Y 27 (1989) 63–70, https://doi.org/10.1016/0008-6223(89)90157-7.

[20] S.S. Barton, M.J.B. Evans, J.A.F. MacDonald, The adsorption of water vapor by porous carbon, Carbon N Y 29 (1991) 1099–1105, https://doi.org/10.1016/0008-6223(91)90026-F.

[21] J. Byun, H.A. Patel, D. Thirion, C.T. Yavuz, Reversible water capture by a charged metal-free porous polymer, Polymer (Guildf) 126 (2017) 308–313, https://doi.org/10.1016/j.polymer.2017.05.071.

[22] L. Jia, X. Yao, J. Ma, C. Long, Adsorption kinetics of water vapor on hypercrosslinked polymeric adsorbent and its comparison with carbonaceous adsorbents, Microporous Mesoporous Mater. 241 (2017) 178–184, https://doi.org/10.1016/j.micromeso.2016.12.028.

[23] M. Sultan, I.I. El-Sharkawy, T. Miyazaki, B.B. Saha, S. Koyama, T. Maruyama, et al., Insights of water vapor sorption onto polymer based sorbents, Adsorption 21 (2015) 205–215, https://doi.org/10.1007/s10450-015-9663-y.

[24] M. Sultan, I.I. El-Sharkawy, T. Miyazaki, B.B. Saha, S. Koyama, T. Maruyama, et al., Water vapor sorption kinetics of polymer based sorbents: theory and experiments, Appl. Therm. Eng. 106 (2016) 192–202, https://doi.org/10.1016/j.applthermaleng.2016.05.192.

[25] S. Hanif, M. Sultan, T. Miyazaki, Effect of relative humidity on thermal conductivity of zeolite-based adsorbents: theory and experiments, Appl. Therm. Eng. 150 (2019) 11–18, https://doi.org/10.1016/j.applthermaleng.2018.12.144.

[26] S.K. Henninger, S.J. Ernst, L. Gordeeva, P. Bendix, D. Fröhlich, A.D. Grekova, et al., New materials for adsorption heat transformation and storage, Renew. Energy 110 (2017) 59–68, https://doi.org/10.1016/j.renene.2016.08.041.

[27] F. Meunier, Second law analysis of a solid adsorption heat pump operating on reversible cascade cycles: application to the zeolite-water pair, J. Heat Recover Syst. 5 (1985) 133–141, https://doi.org/10.1016/0198-7593(85)90045-1.

[28] I. Chandra, V.S. Patwardhan, Theoretical studies on adsorption heat transformer using zeolite-water vapour pair, Heat Recover Syst. CHP 10 (1990) 527–537, https://doi.org/10.1016/0890-4332(90)90203-V.

[29] M. Sultan, T. Miyazaki, B.B. Saha, S. Koyama, Steady-state investigation of water vapor adsorption for thermally driven adsorption based greenhouse air-conditioning system, Renew. Energy 86 (2016) 785–795, https://doi.org/10.1016/j.renene.2015.09.015.

[30] S. Hanif, M. Sultan, T. Miyazaki, S. Koyama, Investigation of energy-efficient solid desiccant system for the drying of wheat grains, Int. J. Agric. Biol. Eng. 12 (2019) 221–228, https://doi.org/10.25165/j.ijabe.20191201.3854.

[31] M.H. Mahmood, M. Sultan, T. Miyazaki, Solid desiccant dehumidification-based air-conditioning system for agricultural storage application: theory and experiments, Proc. Inst. Mech. Eng. A J. Power Energy 095765091986950 (2019), https://doi.org/10.1177/0957650919869503.

[32] K. Lim, J. Che, J. Lee, Experimental study on adsorption characteristics of a water and silica-gel based thermal energy storage (TES) system, Appl. Therm. Eng. 110 (2017) 80–88, https://doi.org/10.1016/j.applthermaleng.2016.08.098.

[33] Z. Lu, R. Wang, Z. Xia, Experimental analysis of an adsorption air conditioning with micro-porous silica gel-water, Appl. Therm. Eng. 50 (2013) 1015–1020, https://doi.org/10.1016/j.applthermaleng.2012.07.041.

[34] E. Passos, F. Meunier, J.C. Gianola, Thermodynamic performance improvement of an intermittent solar-powered refrigeration cycle using adsorption of methanol on activated carbon, J. Heat Recover Syst. 6 (1986) 259–264, https://doi.org/10.1016/0198-7593(86)90010-X.

[35] T.B. Sitorus, F.H. Napitupulu, H. Ambarita, A study on adsorption refrigerator driven by solar collector using Indonesian activated carbon, J. Eng. Technol. Sci. 49 (2018) 657, https://doi.org/10.5614/j.eng.technol.sci.2017.49.5.7.

[36] M.O. Abdullah, I.A.W. Tan, L.S. Lim, Automobile adsorption air-conditioning system using oil palm biomass-based activated carbon: a review, Renew. Sust. Energ. Rev. 15 (2011) 2061–2072, https://doi.org/10.1016/j.rser.2011.01.012.

[37] M. Pons, P. Grenier, Experimental data on a solar-powered ice maker using activated carbon and methanol adsorption pair, J. Sol. Energy Eng. Trans. ASME 109 (1987) 303–310, https://doi.org/10.1115/1.3268222.

[38] M. Sultan, T. Miyazaki, S. Koyama, Z.M. Khan, Performance evaluation of hydrophilic organic polymer sorbents for desiccant air-conditioning applications, Adsorpt. Sci. Technol. 36 (2018) 311–326, https://doi.org/10.1177/0263617417692338.

[39] Y.Z. Lu, R.Z. Wang, M. Zhang, S. Jiangzhou, Adsorption cold storage system with zeolite-water working pair used for locomotive air conditioning, Energy Convers. Manag. 44 (2003) 1733–1743, https://doi.org/10.1016/S0196-8904(02)00169-3.

[40] G. Restuccia, A. Freni, G. Maggio, A zeolite-coated bed for air conditioning adsorption systems: parametric study of heat and mass transfer by dynamic simulation, Appl. Therm. Eng. 22 (2002) 619–630, https://doi.org/10.1016/S1359-4311(01)00114-4.

[41] K.C. Ng, M. Burhan, M.W. Shahzad, Ismail A. Bin, A universal isotherm model to capture adsorption uptake and energy distribution of porous heterogeneous surface, Sci. Rep. 7 (2017) 1–11, https://doi.org/10.1038/s41598-017-11156-6.

[42] J.D. Evans, B. Garai, H. Reinsch, W. Li, S. Dissegna, V. Bon, et al., Metal–organic frameworks in Germany: from synthesis to function, Coord. Chem. Rev. 380 (2019) 378–418, https://doi.org/10.1016/j.ccr.2018.10.002.

[43] H. Li, M. Eddaoudi, M. O'Keeffe, O.M. Yaghi, Design and synthesis of an exceptionally stable and highly porous metal-organic framework, Nature 402 (1999) 276–279, https://doi.org/10.1038/46248.

[44] V.I.J.J. Perry, J.A. Perman, M.J. Zaworotko, Design and synthesis of metal-organic frameworks using metal-organic polyhedra as supermolecular building blocks, Chem. Soc. Rev. 38 (2009) 1400–1417, https://doi.org/10.1039/b807086p.

[45] S.K. Elsaidi, M.H. Mohamed, D. Banerjee, P.K. Thallapally, Flexibility in metal–organic frameworks: a fundamental understanding, Coord. Chem. Rev. 358 (2018) 125–152, https://doi.org/10.1016/j.ccr.2017.11.022.

[46] O.M. Yaghi, M. O'Keeffe, N.W. Ockwig, H.K. Chae, M. Eddaoudi, J. Kim, Reticular synthesis and the design of new materials, Nature 423 (2003) 705–714, https://doi.org/10.1038/nature01650.

[47] Nobar S. Najafi, Cu-BTC synthesis, characterization and preparation for adsorption studies, Mater. Chem. Phys. 213 (2018) 343–351, https://doi.org/10.1016/j.matchemphys.2018.04.031.

[48] M. Alvaro, E. Carbonell, B. Ferrer, I. Llabrés, F.X. Xamena, H. Garcia, Semiconductor behavior of a metal-organic framework (MOF), Chem. - A Eur. J. 13 (2007) 5106–5112, https://doi.org/10.1002/chem.200601003.

[49] E. Elsayed, R. Al-Dadah, S. Mahmoud, A. Elsayed, P.A. Anderson, Aluminium fumarate and CPO-27(Ni) MOFs: characterization and thermodynamic analysis for adsorption heat pump applications, Appl. Therm. Eng. 99 (2016) 802–812, https://doi.org/10.1016/j.applthermaleng.2016.01.129.

[50] E. Elsayed, AL-Dadah R, Mahmoud S, Anderson PA, Elsayed A, Youssef PG., CPO-27(Ni), aluminium fumarate and MIL-101(Cr) MOF materials for adsorption water desalination, Desalination 406 (2017) 25–36, https://doi.org/10.1016/j.desal.2016.07.030.

[51] C.A. Fernandez, P.K. Thallapally, R.K. Motkuri, S.K. Nune, J.C. Sumrak, J. Tian, et al., Gas-induced expansion and contraction of a fluorinated metal-organic framework, Cryst. Growth Des. 10 (2010) 1037–1039, https://doi.org/10.1021/cg9014948.

[52] P.G. Youssef, H. Dakkama, S.M. Mahmoud, AL-Dadah RK., Experimental investigation of adsorption water desalination/cooling system using CPO-27Ni MOF, Desalination 404 (2017) 192–199, https://doi.org/10.1016/j.desal.2016.11.008.

[53] B. Shi, R. Al-Dadah, S. Mahmoud, A. Elsayed, E. Elsayed, CPO-27(Ni) metal-organic framework based adsorption system for automotive air conditioning, Appl. Therm. Eng. 106 (2016) 325–333, https://doi.org/10.1016/j.applthermaleng.2016.05.109.

[54] M. Bahri, F. Haghighat, H. Kazemian, S. Rohani, A comparative study on metal organic frameworks for indoor environment application: adsorption evaluation, Chem. Eng. J. 313 (2017) 711–723, https://doi.org/10.1016/j.cej.2016.10.004.

[55] A. Rezk, R. Al-Dadah, S. Mahmoud, A. Elsayed, Experimental investigation of metal organic frameworks characteristics for water adsorption chillers, Proc. Inst. Mech. Eng. C J. Mech. Eng. Sci. 227 (2013) 992–1005, https://doi.org/10.1177/0954406212456469.

[56] L. Grajciar, O. Bludský, P. Nachtigall, Water adsorption on coordinatively unsaturated sites in CuBTC MOF, J. Phys. Chem. Lett. 1 (2010) 3354–3359, https://doi.org/10.1021/jz101378z.

[57] T. Rajkumar, D. Kukkar, K.H. Kim, J.R. Sohn, A. Deep, Cyclodextrin-metal–organic framework (CD-MOF): from synthesis to applications, J. Ind. Eng. Chem. 72 (2019) 50–66, https://doi.org/10.1016/j.jiec.2018.12.048.

[58] M. Wickenheisser, A. Herbst, R. Tannert, B. Milow, C. Janiak, Hierarchical MOF-xerogel monolith composites from embedding MIL-100(Fe,Cr) and MIL-101(Cr) in resorcinol-formaldehyde xerogels for water adsorption applications, Microporous Mesoporous Mater. 215 (2015) 143–153, https://doi.org/10.1016/j.micromeso.2015.05.017.

[59] M. Wickenheisser, T. Paul, C. Janiak, Prospects of monolithic MIL-MOF@poly (NIPAM)HIPE composites as water sorption materials, Microporous Mesoporous Mater. 220 (2016) 258–269, https://doi.org/10.1016/j.micromeso.2015.09.008.

[60] P. Bareschino, G. Diglio, F. Pepe, G. Angrisani, C. Roselli, M. Sasso, Numerical study of a MIL101 metal organic framework based desiccant cooling system for air conditioning applications, Appl. Therm. Eng. 124 (2017) 641–651, https://doi.org/10.1016/j.applthermaleng.2017.06.024.

[61] J.A. Greathouse, M.D. Allendorf, The interaction of water with MOF-5 simulated by molecular dynamics, J. Am. Chem. Soc. 128 (2006) 10678–10679, https://doi.org/10.1021/ja063506b.

[62] Y. Ming, N. Kumar, D.J. Siegel, Water adsorption and insertion in MOF-5, ACS Omega 2 (2017) 4921–4928, https://doi.org/10.1021/acsomega.7b01129.

[63] Chui SSY, Lo SMF, Charmant JPH, A.G. Orpen, I.D. Williams, A chemically functionalizable nanoporous material [Cu_3(TMA)_2(H_2O)_3]_n, Science (80-) 283 (1999) 1148–1150, https://doi.org/10.1126/science.283.5405.1148.

[64] M. Díaz-garcía, M. Sánchez-sánchez, Microporous and mesoporous materials synthesis and characterization of a new Cd-based metal-organic framework isostructural with MOF-74 / CPO-27 materials 190 (2014) 248–254, https://doi.org/10.1016/j.micromeso.2014.02.021.

[65] J. Liu, Y. Wang, A.I. Benin, P. Jakubczak, R.R. Willis, M.D. LeVan, CO2/H2O adsorption equilibrium and rates on metal-organic frameworks: HKUST-1 and Ni/DOBDC, Langmuir 26 (2010) 14301–14307, https://doi.org/10.1021/la102359q.

[66] H.W.B. Teo, A. Chakraborty, Water adsorption on various metal organic framework, IOP Conf. Ser. Mater. Sci. Eng. 272 (2017), 012019, https://doi.org/10.1088/1757-899X/272/1/012019.

[67] L.G. Gordeeva, M.V. Solovyeva, Y.I. Aristov, NH2-MIL-125 as a promising material for adsorptive heat transformation and storage, Energy 100 (2016) 18–24, https://doi.org/10.1016/j.energy.2016.01.034.

[68] H. Furukawa, F. Gándara, Y.-B. Zhang, J. Jiang, W.L. Queen, M.R. Hudson, et al., Water adsorption in porous metal–organic frameworks and related materials, J. Am. Chem. Soc. 136 (2014) 4369–4381, https://doi.org/10.1021/ja500330a.

[69] V. Bon, I. Senkovska, J.D. Evans, M. Wöllner, M. Hölzel, S. Kaskel, Insights into the water adsorption mechanism in the chemically stable zirconium-based MOF DUT-67-a prospective material for adsorption-driven heat transformations, J. Mater. Chem. A 7 (2019) 12681–12690, https://doi.org/10.1039/c9ta00825j.
[70] S. Arh, B. Gašperšič, Development and comparison of different advanced absorption cycles, Int. J. Refrig. 13 (1990) 41–50, https://doi.org/10.1016/0140-7007(90)90053-Y.
[71] M.V. Solovyeva, Y.I. Aristov, L.G. Gordeeva, NH2-MIL-125 as promising adsorbent for adsorptive cooling: water adsorption dynamics, Appl. Therm. Eng. 116 (2017) 541–548, https://doi.org/10.1016/j.applthermaleng.2017.01.080.
[72] M. Tatlier, Performances of MOF vs. zeolite coatings in adsorption cooling applications, Appl. Therm. Eng. 113 (2017) 290–297, https://doi.org/10.1016/j.applthermaleng.2016.10.189.
[73] H. Kummer, M. Baumgartner, P. Hïgenell, D. Frïhlich, S.K. Henninger, R. Glïser, Thermally driven refrigeration by methanol adsorption on coatings of HKUST-1 and MIL-101(Cr), Appl. Therm. Eng. 117 (2017) 689–697, https://doi.org/10.1016/j.applthermaleng.2016.11.026.
[74] J.J. Jenks, R.K. Motkuri, W. TeGrotenhuis, B.K. Paul, B.P. McGrail, Simulation and experimental study of metal organic frameworks used in adsorption cooling, Heat Transf. Eng. 38 (2017) 1305–1315, https://doi.org/10.1080/01457632.2016.1242965.
[75] L. Ma, Z. Rui, Q. Wu, H. Yang, Y. Yin, Z. Liu, et al., Performance evaluation of shaped MIL-101-ethanol working pair for adsorption refrigeration, Appl. Therm. Eng. 95 (2016) 223–228, https://doi.org/10.1016/j.applthermaleng.2015.09.023.
[76] A. Rezk, AL-Dadah R, Mahmoud S, Elsayed A., Investigation of ethanol/metal organic frameworks for low temperature adsorption cooling applications, Appl. Energy 112 (2013) 1025–1031, https://doi.org/10.1016/j.apenergy.2013.06.041.
[77] B.B. Saha, I.I. El-Sharkawy, T. Miyazaki, S. Koyama, S.K. Henninger, A. Herbst, et al., Ethanol adsorption onto metal organic framework: theory and experiments, Energy 79 (2015) 363–370, https://doi.org/10.1016/j.energy.2014.11.022.
[78] W. Li, X. Xia, M. Cao, S. Li, Structure-property relationship of metal-organic frameworks for alcohol-based adsorption-driven heat pumps via high-throughput computational screening, J. Mater. Chem. A 7 (2019) 7470–7479, https://doi.org/10.1039/C8TA07909A.
[79] M. Sultan, M.H. Mahmood, T. Miyazaki, S. Koyama, Z.M. Khan, Close and open cycle adsorption kinetics: development of correlation for desiccant air-conditioning, J. Eng. Appl. Sci. 35 (2016) 1–8.
[80] N.C. Burtch, H. Jasuja, K.S. Walton, Water stability and adsorption in metal-organic frameworks, Chem. Rev. 114 (2014) 10575–10612, https://doi.org/10.1021/cr5002589.
[81] H.J. Dakkama, P.G. Youssef, R.K. Al-Dadah, S. Mahmoud, Adsorption ice making and water desalination system using metal organic frameworks/water pair, Energy Convers. Manag. 142 (2017) 53–61, https://doi.org/10.1016/j.enconman.2017.03.036.
[82] M.V. Solovyeva, L.G. Gordeeva, T.A. Krieger, Y.I. Aristov, MOF-801 as a promising material for adsorption cooling: equilibrium and dynamics of water adsorption, Energy Convers. Manag. 174 (2018) 356–363, https://doi.org/10.1016/j.enconman.2018.08.032.
[83] A. Khutia, H.U. Rammelberg, T. Schmidt, S. Henninger, C. Janiak, Water sorption cycle measurements on functionalized MIL-101Cr for heat transformation application, Chem. Mater. 25 (2013) 790–798, https://doi.org/10.1021/cm304055k.
[84] E. Hastürk, S.J. Ernst, C. Janiak, Recent advances in adsorption heat transformation focusing on the development of adsorbent materials, Curr. Opin. Chem. Eng. 24 (2019) 26–36, https://doi.org/10.1016/j.coche.2018.12.011.
[85] P. D'Ans, E. Courbon, A. Permyakova, F. Nouar, C. Simonnet-Jégat, F. Bourdreux, et al., A new strontium bromide MOF composite with improved performance for solar energy storage application, J. Energy Storage 25 (2019) 100881, https://doi.org/10.1016/j.est.2019.100881.
[86] M. Qin, P. Hou, Z. Wu, J. Wang, Precise humidity control materials for autonomous regulation of indoor moisture, Build. Environ. 106581 (2019), https://doi.org/10.1016/j.buildenv.2019.106581.
[87] B. Shi, Development of an MOF Based Adsorption Air Conditioning System for Automotive Application, 2015.
[88] R.J. Drout, L. Robison, Z. Chen, T. Islamoglu, O.K. Farha, Zirconium metal–organic frameworks for organic pollutant adsorption, Trends Chem 1 (2019) 304–317, https://doi.org/10.1016/j.trechm.2019.03.010.
[89] H. Kim, S. Yang, S.R. Rao, S. Narayanan, E.A. Kapustin, H. Furukawa, et al., Water harvesting from air with metal-organic frameworks powered by natural sunlight, Science (80-) 356 (2017) 430–434, https://doi.org/10.1126/science.aam8743.
[90] A. Entezari, M. Ejeian, R. Wang, Modifying water sorption properties with polymer additives for atmospheric water harvesting applications, Appl. Therm. Eng. 161 (2019) 114109, https://doi.org/10.1016/j.applthermaleng.2019.114109.
[91] A. Weiss, N. Reimer, N. Stock, M. Tiemann, T. Wagner, Screening of mixed-linker CAU-10 MOF materials for humidity sensing by impedance spectroscopy, Microporous Mesoporous Mater. 220 (2016) 39–43, https://doi.org/10.1016/j.micromeso.2015.08.020.
[92] S. Karmakar, J. Dechnik, C. Janiak, S. De, Aluminium fumarate metal-organic framework: A super adsorbent for fluoride from water, J. Hazard. Mater. 303 (2016) 10–20, https://doi.org/10.1016/j.jhazmat.2015.10.030.
[93] K.Y.A. Lin, Y.T. Liu, S.Y. Chen, Adsorption of fluoride to UiO-66-NH<inf>2</inf> in water: stability, kinetic, isotherm and thermodynamic studies, J. Colloid Interface Sci. 461 (2016) 79–87, https://doi.org/10.1016/j.jcis.2015.08.061.
[94] J. Yan, Y. Yu, C. Ma, J. Xiao, Q. Xia, Y. Li, et al., Adsorption isotherms and kinetics of water vapor on novel adsorbents MIL-101(Cr)@GO with super-high capacity, Appl. Therm. Eng. 84 (2015) 118–125, https://doi.org/10.1016/j.applthermaleng.2015.03.040.
[95] G. Férey, C. Mellot-Draznieks, C. Serre, F. Millange, J. Dutour, S. Surblé, et al., A chromium terephthalate – based solid with unusually large pore volumes and surface area, Science (80-) 309 (2005) 2040–2042, https://doi.org/10.1126/science.1116275.
[96] F. Jeremias, D. Fröhlich, C. Janiak, S.K. Henninger, Advancement of sorption-based heat transformation by a metal coating of highly-stable, hydrophilic aluminium fumarate MOF, RSC Adv. 4 (2014) 24073–24082, https://doi.org/10.1039/c4ra03794d.
[97] F. Jeremias, A. Khutia, S.K. Henninger, C. Janiak, MIL-100(Al, Fe) as water adsorbents for heat transformation purposes - a promising application, J. Mater. Chem. 22 (2012) 10148–10151, https://doi.org/10.1039/c2jm15615f.
[98] M. Wickenheisser, F. Jeremias, S.K. Henninger, C. Janiak, Grafting of hydrophilic ethylene glycols or ethylenediamine on coordinatively unsaturated metal sites in MIL-100(Cr) for improved water adsorption characteristics, Inorg. Chim. Acta 407 (2013) 145–152, https://doi.org/10.1016/j.ica.2013.07.024.
[99] F. Jeremias, V. Lozan, S.K. Henninger, C. Janiak, Programming MOFs for water sorption: amino-functionalized MIL-125 and UiO-66 for heat transformation and heat storage applications, Dalton Trans. 42 (2013) 15967–15973, https://doi.org/10.1039/c3dt51471d.
[100] S.N. Kim, J. Kim, H.Y. Kim, H.Y. Cho, W.S. Ahn, Adsorption/catalytic properties of MIL-125 and NH2-MIL-125, Catal. Today 204 (2013) 85–93, https://doi.org/10.1016/j.cattod.2012.08.014.
[101] M. Sindoro, A.Y. Jee, S. Granick, Shape-selected colloidal MOF crystals for aqueous use, Chem. Commun. 49 (2013) 9576–9578, https://doi.org/10.1039/c3cc45935g.
[102] D. Cunha, M. Ben Yahia, S. Hall, S.R. Miller, H. Chevreau, E. Elkaïm, et al., Rationale of drug encapsulation and release from biocompatible porous metal-organic frameworks, Chem. Mater. 25 (2013) 2767–2776, https://doi.org/10.1021/cm400798p.
[103] S.M. Towsif Abtab, D. Alezi, P.M. Bhatt, A. Shkurenko, Y. Belmabkhout, H. Aggarwal, et al., Reticular chemistry in action: a hydrolytically stable MOF capturing twice its weight in adsorbed water, Chem 4 (2018) 94–105, https://doi.org/10.1016/j.chempr.2017.11.005.
[104] D.J. Tranchemontagne, J.R. Hunt, O.M. Yaghi, Room temperature synthesis of metal-organic frameworks: MOF-5, MOF-74, MOF-177, MOF-199, and IRMOF-0, Tetrahedron 64 (2008) 8553–8557, https://doi.org/10.1016/j.tet.2008.06.036.
[105] J.R. Karra, B.E. Grabicka, Y.G. Huang, K.S. Walton, Adsorption study of CO2, CH4, N2, and H2O on an interwoven copper carboxylate metal-organic framework (MOF-14), J. Colloid Interface Sci. 392 (2013) 331–336, https://doi.org/10.1016/j.jcis.2012.10.018.
[106] Z. Zhao, S. Wang, Y. Yang, X. Li, J. Li, Z. Li, Competitive adsorption and selectivity of benzene and water vapor on the microporous metal organic frameworks (HKUST-1), Chem. Eng. J. 259 (2015) 79–89, https://doi.org/10.1016/j.cej.2014.08.012.
[107] F. Bonino, S. Chavan, J.G. Vitillo, E. Groppo, G. Agostini, C. Lamberti, et al., Local structure of CPO-27-Ni metallorganic framework upon dehydration and coordination of NO, Chem. Mater. 20 (2008) 4957–4968, https://doi.org/10.1021/cm800686k.
[108] Y. Jiao, C.R. Morelock, N.C. Burtch, W.P. Mounfield, J.T. Hungerford, K. S. Walton, Tuning the kinetic water stability and adsorption interactions of mg-MOF-74 by partial substitution with co or Ni, Ind. Eng. Chem. Res. 54 (2015) 12408–12414, https://doi.org/10.1021/acs.iecr.5b03843.
[109] J.D. Howe, C.R. Morelock, Y. Jiao, K.W. Chapman, K.S. Walton, D.S. Sholl, Understanding structure, metal distribution, and water adsorption in mixed-metal MOF-74, J. Phys. Chem. C 121 (2017) 627–635, https://doi.org/10.1021/acs.jpcc.6b11719.
[110] E. Haque, S.H. Jhung, Synthesis of isostructural metal-organic frameworks, CPO-27s, with ultrasound, microwave, and conventional heating: effect of synthesis methods and metal ions, Chem. Eng. J. 173 (2011) 866–872, https://doi.org/10.1016/j.cej.2011.08.037.
[111] T. Xiao, D. Liu, The most advanced synthesis and a wide range of applications of MOF-74 and its derivatives, Microporous Mesoporous Mater. 283 (2019) 88–103, https://doi.org/10.1016/j.micromeso.2019.03.002.
[112] H. Reinsch, M.A. Van Der Veen, B. Gil, B. Marszalek, T. Verbiest, D. De Vos, et al., Structures, sorption characteristics, and nonlinear optical properties of a new series of highly stable aluminum MOFs, Chem. Mater. 25 (2013) 17–26, https://doi.org/10.1021/cm3025445.
[113] A. Schaate, P. Roy, T. Preuße, S.J. Lohmeier, A. Godt, P. Behrens, Porous interpenetrated zirconium-organic frameworks (PIZOFs): a chemically versatile family of metal-organic frameworks, Chem. - A Eur. J. 17 (2011) 9320–9325, https://doi.org/10.1002/chem.201101015.
[114] P. Roy, A. Schaate, P. Behrens, A. Godt, Post-synthetic modification of Zr-metal-organic frameworks through cycloaddition reactions, Chem. - A Eur. J. 18 (2012) 6979–6985, https://doi.org/10.1002/chem.201103288.
[115] A. Schaate, P. Roy, A. Godt, J. Lippke, F. Waltz, M. Wiebcke, et al., Modulated synthesis of Zr-based metal-organic frameworks: from nano to single crystals, Chem. - A Eur. J. 17 (2011) 6643–6651, https://doi.org/10.1002/chem.201003211.
[116] D. Cunha, C. Gaudin, I. Colinet, P. Horcajada, G. Maurin, C. Serre, Rationalization of the entrapping of bioactive molecules into a series of functionalized porous zirconium terephthalate MOFs, J. Mater. Chem. B 1 (2013) 1101–1108, https://doi.org/10.1039/c2tb00366j.

[117] J.H. Cavka, S. Jakobsen, U. Olsbye, N. Guillou, C. Lamberti, S. Bordiga, et al., A new zirconium inorganic building brick forming metal organic frameworks with exceptional stability, J. Am. Chem. Soc. 130 (2008) 13850–13851, https://doi.org/10.1021/ja8057953.
[118] C. Gaudin, D. Cunha, E. Ivanoff, P. Horcajada, G. Chevé, A. Yasri, et al., A quantitative structure activity relationship approach to probe the influence of the functionalization on the drug encapsulation of porous metal-organic frameworks, Microporous Mesoporous Mater. 157 (2012) 124–130, https://doi.org/10.1016/j.micromeso.2011.06.011.
[119] V. Bon, I. Senkovska, I.A. Baburin, S. Kaskel, Zr and Hf based metal-organic frameworks: tracking down the polymorphism, Cryst. Growth Des. 13 (2013) 1231–1237, https://doi.org/10.1021/cg301691d.
[120] A. Perea-Cachero, J. Dechnik, R. Lahoz, C. Janiak, C. Téllez, J. Coronas, HKUST-1 coatings on laser-microperforated brass supports for water adsorption, CrystEngComm 19 (2017) 1470–1478, https://doi.org/10.1039/c6ce02490d.
[121] J. Canivet, A. Fateeva, Y. Guo, B. Coasne, D. Farrusseng, Water adsorption in MOFs: fundamentals and applications, Chem. Soc. Rev. 43 (2014) 5594–5617, https://doi.org/10.1039/c4cs00078a.
[122] K. Lee, J.D. Howe, L.C. Lin, B. Smit, J.B. Neaton, Small-molecule adsorption in open-site metal-organic frameworks: A systematic density functional theory study for rational design, Chem. Mater. 27 (2015) 668–678, https://doi.org/10.1021/cm502760q.
[123] M.I. Nandasiri, S.R. Jambovane, B.P. McGrail, H.T. Schaef, S.K. Nune, Adsorption, separation, and catalytic properties of densified metal-organic frameworks, Coord. Chem. Rev. 311 (2016) 38–52, https://doi.org/10.1016/j.ccr.2015.12.004.
[124] D. Fröhlich, E. Pantatosaki, P.D. Kolokathis, K. Markey, H. Reinsch, M. Baumgartner, et al., Water adsorption behaviour of CAU-10-H: A thorough investigation of its structure-property relationships, J. Mater. Chem. A 4 (2016) 11859–11869, https://doi.org/10.1039/c6ta01757f.
[125] E. Flage-Larsen, A. Ryset, J.H. Cavka, K. Thorshaug, Band gap modulations in UiO metal-organic frameworks, J. Phys. Chem. C 117 (2013) 20610–20616, https://doi.org/10.1021/jp405335q.
[126] H. Reinsch, D. De Vos, Structures and properties of gallium-MOFs with MIL-53-topology based on aliphatic linker molecules, Microporous Mesoporous Mater. 200 (2014) 311–316, https://doi.org/10.1016/j.micromeso.2014.07.058.
[127] A. Boutin, D. Bousquet, A.U. Ortiz, F.X. Coudert, A.H. Fuchs, A. Ballandras, et al., Temperature-induced structural transitions in the gallium-based MIL-53 metal-organic framework, J. Phys. Chem. C 117 (2013) 8180–8188, https://doi.org/10.1021/jp312179e.
[128] G. Weber, I. Bezverkhyy, J.P. Bellat, A. Ballandras, G. Ortiz, G. Chaplais, et al., Mechanism of water adsorption in the large pore form of the gallium-based MIL-53 metal-organic framework, Microporous Mesoporous Mater. 222 (2016) 145–152, https://doi.org/10.1016/j.micromeso.2015.10.003.
[129] R. Al-Dadah, S. Mahmoud, E. Elsayed, P. Youssef, F. Al-Mousawi, Metal-organic framework materials for adsorption heat pumps, Energy 116356 (2019), https://doi.org/10.1016/j.energy.2019.116356.
[130] F.X. Coudert, A.U. Ortiz, V. Haigis, D. Bousquet, A.H. Fuchs, A. Ballandras, et al., Water adsorption in flexible gallium-based MIL-53 metal-organic framework, J. Phys. Chem. C 118 (2014) 5397–5405, https://doi.org/10.1021/jp412433a.
[131] G. Akiyama, R. Matsuda, H. Sato, A. Hori, M. Takata, S. Kitagawa, Effect of functional groups in MIL-101 on water sorption behavior, Microporous Mesoporous Mater. 157 (2012) 89–93, https://doi.org/10.1016/j.micromeso.2012.01.015.
[132] P. Küsgens, M. Rose, I. Senkovska, H. Fröde, A. Henschel, S. Siegle, et al., Characterization of metal-organic frameworks by water adsorption, Microporous Mesoporous Mater. 120 (2009) 325–330, https://doi.org/10.1016/j.micromeso.2008.11.020.
[133] H. Kim, S.R. Rao, E.A. Kapustin, L. Zhao, S. Yang, O.M. Yaghi, et al., Adsorption-based atmospheric water harvesting device for arid climates, Nat. Commun. 9 (2018) 1–8, https://doi.org/10.1038/s41467-018-03162-7.
[134] J. Ehrenmann, S.K. Henninger, C. Janiak, Water adsorption characteristics of MIL-101 for heat-transformation applications of MOFs, Eur. J. Inorg. Chem. (2011) 471–474, https://doi.org/10.1002/ejic.201001156.
[135] F. Meunier, Adsorption heat powered heat pumps, Appl. Therm. Eng. 61 (2013) 830–836, https://doi.org/10.1016/j.applthermaleng.2013.04.050.
[136] W.S. Chang, C.C. Wang, C.C. Shieh, Experimental study of a solid adsorption cooling system using flat-tube heat exchangers as adsorption bed, Appl. Therm. Eng. 27 (2007) 2195–2199, https://doi.org/10.1016/j.applthermaleng.2005.07.022.
[137] Y. Liu, K.C. Leong, Numerical study of a novel cascading adsorption cycle, Int. J. Refrig. 29 (2006) 250–259, https://doi.org/10.1016/j.ijrefrig.2005.05.008.
[138] T.F. Qu, R.Z. Wang, W. Wang, Study on heat and mass recovery in adsorption refrigeration cycles, Appl. Therm. Eng. 21 (2001) 439–452, https://doi.org/10.1016/S1359-4311(00)00050-8.
[139] B.B. Saha, A. Akisawa, T. Kashiwagi, Solar/waste heat driven two-stage adsorption chiller: the prototype, Renew. Energy 23 (2001) 93–101, https://doi.org/10.1016/S0960-1481(00)00107-5.
[140] R.Z. Wang, Performance improvement of adsorption cooling by heat and mass recovery operation, Int. J. Refrig. 24 (2001) 602–611, https://doi.org/10.1016/S0140-7007(01)00004-4.
[141] R.E. Critoph, Forced convection adsorption cycles, Appl. Therm. Eng. 18 (1998) 799–807, https://doi.org/10.1016/s1359-4311(97)00110-5.
[142] S.V. Shelton, W.J. Wepfer, D.J. Miles, Square wave analysis of the solid-vapor adsorption heat pump, Heat Recover Syst. CHP 9 (1989) 233–247, https://doi.org/10.1016/0890-4332(89)90007-0.
[143] P. Reviewed, L. Berkeley, B. Cancer, Lawrence Berkeley National Laboratory Lawrence Berkeley National Laboratory, 2010, pp. 35–43.
[144] R.E. Critoph, Performance limitations of adsorption cycles for solar cooling, Sol. Energy 41 (1988) 21–31, https://doi.org/10.1016/0038-092X(88)90111-9.
[145] A.A. Askalany, M. Salem, I.M. Ismail, A.H.H. Ali, M.G. Morsy, A review on adsorption cooling systems with adsorbent carbon, Renew. Sust. Energ. Rev. 16 (2012) 493–500, https://doi.org/10.1016/j.rser.2011.08.013.
[146] A.N. Shmroukh, A.H.H. Ali, S. Ookawara, Adsorption working pairs for adsorption cooling chillers: A review based on adsorption capacity and environmental impact, Renew. Sust. Energ. Rev. 50 (2015) 445–456, https://doi.org/10.1016/j.rser.2015.05.035.
[147] S. Ülkü, Adsorption heat pumps, J. Heat Recover Syst. 6 (1986) 277–284, https://doi.org/10.1016/0198-7593(86)90113-X.
[148] D. Lenzen, J. Zhao, S.J. Ernst, M. Wahiduzzaman, A. Ken Inge, D. Fröhlich, et al., A metal–organic framework for efficient water-based ultra-low-temperature-driven cooling, Nat. Commun. 10 (2019), https://doi.org/10.1038/s41467-019-10960-0.
[149] S. Alrsheedi, B.B. Saha, A. Chakraborty, S. Alrsheedi, B.B. Saha, A. Chakraborty, et al., Performance Investigation of MOF-Ethanol Based Adsorption Cooling Cycle Carbon dioxide adsorption onto activated carbons View project Dew point evaporative cooling View project Performance Investigation of MOF-Ethanol Based Adsorption Cooling Cycle, 2016.
[150] K. Zu, S. Cui, M. Qin, Performance comparison between metal-organic framework (MOFs) and conventional desiccants (silica gel, zeolite) for a novel high temperature cooling system, IOP Conf. Ser. Mater. Sci. Eng. 609 (2019), https://doi.org/10.1088/1757-899X/609/5/052013. Institute of Physics Publishing.
[151] D. Charoensupaya, W.M. Worek, Parametric study of an open-cycle adiabatic, solid, desiccant cooling system, Energy 13 (1988) 739–747. https://doi.org/10.1016/0360-5442(88)90106-5.
[152] F. Xu, Z.F. Bian, T.S. Ge, Y.J. Dai, C.H. Wang, S. Kawi, Analysis on solar energy powered cooling system based on desiccant coated heat exchanger using metal-organic framework 177 (2019) 211–221, https://doi.org/10.1016/j.energy.2019.04.090.
[153] E. Motoasca, Energy Sustainability in Built and Urban Environments, 2019, https://doi.org/10.1007/978-981-13-3284-5.
[154] K.C. Ng, M.W. Shahzad, Sustainable desalination using ocean thermocline energy, Renew. Sust. Energ. Rev. 82 (2018) 240–246, https://doi.org/10.1016/j.rser.2017.08.087.
[155] M.W. Shahzad, M. Burhan, K.C. Ng, Pushing desalination recovery to the maximum limit: membrane and thermal processes integration, Desalination 416 (2017) 54–64, https://doi.org/10.1016/j.desal.2017.04.024.
[156] M.W. Shahzad, M. Burhan, L. Ang, K.C. Ng, Energy-water-environment nexus underpinning future desalination sustainability, Desalination 413 (2017) 52–64, https://doi.org/10.1016/j.desal.2017.03.009.
[157] S. Mitra, K. Thu, B.B. Saha, K. Srinivasan, P. Dutta, Modeling study of two-stage, multi-bed air cooled silica gel + water adsorption cooling cum desalination system, Appl. Therm. Eng. 114 (2017) 704–712, https://doi.org/10.1016/j.applthermaleng.2016.12.011.
[158] K. Yang, Y. Shi, M. Wu, W. Wang, Y. Jin, R. Li, et al., Hollow spherical SiO_2 micro-container encapsulation of LiCl for high-performance simultaneous heat reallocation and seawater desalination, J. Mater. Chem. A (2020), https://doi.org/10.1039/C9TA11721K.
[159] M.W. Shahzad, K.C. Ng, K. Thu, Future sustainable desalination using waste heat: kudos to thermodynamic synergy, Environ. Sci. Water Res. Technol. 2 (2016) 206–212, https://doi.org/10.1039/c5ew00217f.
[160] B.B. Saha, I.I. El-Sharkawy, M.W. Shahzad, K. Thu, L. Ang, K.C. Ng, Fundamental and application aspects of adsorption cooling and desalination, Appl. Therm. Eng. 97 (2016) 68–76, https://doi.org/10.1016/j.applthermaleng.2015.09.113.
[161] K. Thu, Y.D. Kim, M.W. Shahzad, J. Saththasivam, K.C. Ng, Performance investigation of an advanced multi-effect adsorption desalination (MEAD) cycle, Appl. Energy 159 (2015) 469–477, https://doi.org/10.1016/j.apenergy.2015.09.035.
[162] M.W. Shahzad, K. Thu, Kim Y. Deuk, K.C. Ng, An experimental investigation on MEDAD hybrid desalination cycle, Appl. Energy 148 (2015) 273–281, https://doi.org/10.1016/j.apenergy.2015.03.062.
[163] K.C. Ng, K. Thu, S.J. Oh, L. Ang, M.W. Shahzad, Ismail A. Bin, Recent developments in thermally-driven seawater desalination: energy efficiency improvement by hybridization of the MED and AD cycles, Desalination 356 (2015) 255–270, https://doi.org/10.1016/j.desal.2014.10.025.
[164] M.W. Shahzad, K.C. Ng, K. Thu, B.B. Saha, W.G. Chun, Multi effect desalination and adsorption desalination (MEDAD): A hybrid desalination method, Appl. Therm. Eng. 72 (2014) 289–297, https://doi.org/10.1016/j.applthermaleng.2014.03.064.
[165] K.C. Ng, K. Thu, M.W. Shahzad, W. Chun, Progress of adsorption cycle and its hybrids with conventional multi-effect desalination processes, IDA J Desalin Water Reuse 6 (2014) 44–56, https://doi.org/10.1179/2051645214y.0000000020.
[166] H.S. Son, M.W. Shahzad, N. Ghaffour, K.C. Ng, Pilot studies on synergetic impacts of energy utilization in hybrid desalination system: multi-effect distillation and adsorption cycle (MED-AD), Desalination 477 (2020), https://doi.org/10.1016/j.desal.2019.114266.
[167] P. Youssef, S. Mahmoud, R. Al-Dadah, E. Elsayed, O. El-Samni, Numerical investigation of aluminum fumarate MOF adsorbent material for adsorption desalination/cooling application, Energy Procedia 142 (2017) 1693–1698, https://doi.org/10.1016/j.egypro.2017.12.551.

[168] R. Hollman, W.A. Little, Progress in the development of microminiature refrigerators using photolithographic fabrication techniques, Proceedings of the Conference on Refrigeration for Cryogenic Sensors and Electronic Systems, U.S. Department of Commerce / National Bureau of Standards, Boulder, CO (1980) 160–163.

[169] E.E. Anyanwu, Review of solid adsorption solar refrigeration II:: an overview of the principles and theory, Energy Convers. Manag. 45 (2004) 1279–1295, https://doi.org/10.1016/j.enconman.2003.08.003.

[170] B.B. Saha, E.C. Boelman, T. Kashiwagi, Computational analysis of an advanced adsorption-refrigeration cycle, Energy 20 (1995) 983–994, https://doi.org/10.1016/0360-5442(95)00047-K.

[171] S.K. Henninger, F.P. Schmidt, H.M. Henning, Water adsorption characteristics of novel materials for heat transformation applications, Appl. Therm. Eng. 30 (2010) 1692–1702, https://doi.org/10.1016/j.applthermaleng.2010.03.028.

[172] S.K. Henninger, H.A. Habib, C. Janiak, MOFs as adsorbents for low temperature heating and cooling applications, J. Am. Chem. Soc. 131 (2009) 2776–2777, https://doi.org/10.1021/ja808444z.